

REVIEW PAPER

# From proto-Kranz to C<sub>4</sub> Kranz: building the bridge to C<sub>4</sub> photosynthesis

Rowan F. Sage, Roxana Khoshnavesh and Tammy L. Sage\*

Department of Ecology and Evolutionary Biology, The University of Toronto, 25 Willcocks Street, Toronto, On M5S3B2 Canada

\* To whom correspondence should be addressed. E-mail: [tammy.sage@utoronto.ca](mailto:tammy.sage@utoronto.ca)

Received 2 January 2014; Revised 14 March 2014; Accepted 24 March 2014

## Abstract

In this review, we examine how the specialized “Kranz” anatomy of C<sub>4</sub> photosynthesis evolved from C<sub>3</sub> ancestors. Kranz anatomy refers to the wreath-like structural traits that compartmentalize the biochemistry of C<sub>4</sub> photosynthesis and enables the concentration of CO<sub>2</sub> around Rubisco. A simplified version of Kranz anatomy is also present in the species that utilize C<sub>2</sub> photosynthesis, where a photorespiratory glycine shuttle concentrates CO<sub>2</sub> into an inner bundle-sheath-like compartment surrounding the vascular tissue. C<sub>2</sub> Kranz is considered to be an intermediate stage in the evolutionary development of C<sub>4</sub> Kranz, based on the intermediate branching position of C<sub>2</sub> species in 14 evolutionary lineages of C<sub>4</sub> photosynthesis. In the best-supported model of C<sub>4</sub> evolution, Kranz anatomy in C<sub>2</sub> species evolved from C<sub>3</sub> ancestors with enlarged bundle sheath cells and high vein density. Four independent lineages have been identified where C<sub>3</sub> sister species of C<sub>2</sub> plants exhibit an increase in organelle numbers in the bundle sheath and enlarged bundle sheath cells. Notably, in all of these species, there is a pronounced shift of mitochondria to the inner bundle sheath wall, forming an incipient version of the C<sub>2</sub> type of Kranz anatomy. This incipient version of C<sub>2</sub> Kranz anatomy is termed proto-Kranz, and is proposed to scavenge photorespiratory CO<sub>2</sub>. By doing so, it may provide fitness benefits in hot environments, and thus represent a critical first stage of the evolution of both the C<sub>2</sub> and C<sub>4</sub> forms of Kranz anatomy.

**Key words:** C<sub>4</sub> evolution, C<sub>2</sub> photosynthesis, C<sub>4</sub> photosynthesis, C<sub>3</sub>–C<sub>4</sub> intermediate, glycine shuttle, Kranz anatomy, photorespiration, proto-Kranz anatomy.

## Introduction

A major feature of C<sub>4</sub> photosynthesis is the specialization of leaf structure to form Kranz anatomy, wherein CO<sub>2</sub> is first assimilated by PEPcase in a layer of mesophyll (M) cells that surround an inner layer of bundle-sheath-like Kranz (K) cells, where CO<sub>2</sub> is concentrated and refixed by Rubisco (Fig. 1; Brown, 1975). Of the 65 to 70 known lineages of C<sub>4</sub> plants (Sage *et al.*, 2011a, 2012), only a few lack Kranz anatomy. These are the single-celled C<sub>4</sub> plants occurring in two terrestrial C<sub>4</sub> lineages of the Chenopodiaceae, a C<sub>4</sub> lineage of diatoms, and two lineages in the Hydrocharitaceae, a family of aquatic angiosperms (Bowes, 2011; Edwards and Voznesenskaya, 2011; Sage *et al.* 2011a). In terrestrial plants, variants of C<sub>4</sub>-Kranz anatomy have independently evolved at

least 60 times, making the Kranz syndrome one of the most convergent structural types in the living world (Sage *et al.* 2011a; Edwards and Voznesenskaya, 2011).

Kranz anatomy encompasses many distinct forms (Hattersley and Watson, 1992; Edwards and Voznesenskaya, 2011; Kadereit *et al.*, 2012; Freitag and Kadereit, 2013). The inner layer of K cells can be derived from parenchymatous bundle sheath (eudicots and many monocots), a mestome sheath around the vascular bundle (monocots only), or a sheath of parenchymatous cells around layers of water storage cells (eudicots only; Brown, 1975; Dengler and Nelson, 1999; Edwards and Voznesenskaya, 2011; see Supplementary Figs S1, S2 for examples). Kranz cells are generally more

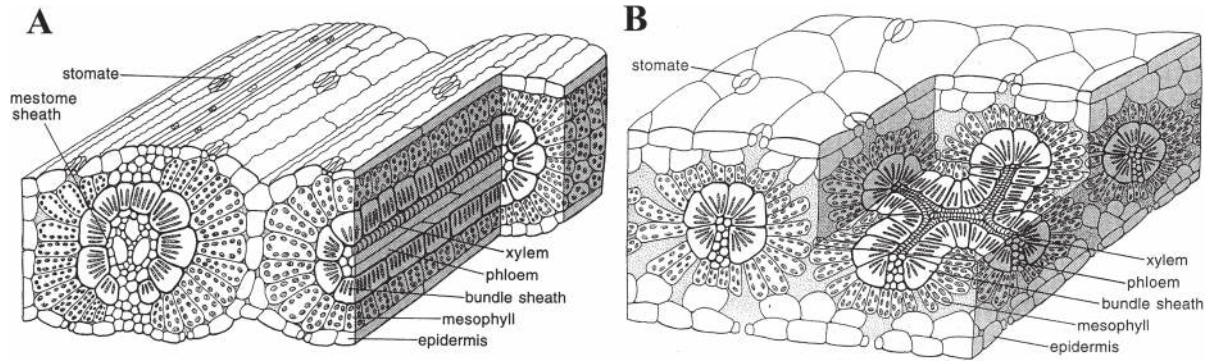


**Fig. 1.** Diagrams of classical forms of  $C_4$  Kranz anatomy drawn from (A) an NAD-malic enzyme type of  $C_4$  grass (*Panicum capillare*) and (B) the NAD-malic enzyme type of  $C_4$  eudicot *Atriplex rosea*. Note the radial arrangement of a single layer of mesophyll cells around a layer of parenchymatous bundle sheath cells, and the presence of a mestome sheath in the larger veins of the  $C_4$  grass in panel A. See [Supplementary Fig. S1](#) for micrographs of numerous  $C_4$  Kranz types, including *A. rosea*. Reprinted from Dengler NG, Nelson T. 1999. Leaf structure and development in  $C_4$  plants. In: Sage R, Monson R, eds.  *$C_4$  plant biology*. San Diego: Academic Press, 133–172. [www.elsevier.com](http://www.elsevier.com).

conspicuous than the homologous cells of their  $C_3$  relatives, owing to the presence of larger and more numerous chloroplasts, thick outer walls, tight packing around the vascular bundles or water-storage cells, and limited exposure to intercellular air spaces (Fig. 1, [Supplementary Figs S1, S2](#); Brown, 1977; Hattersley and Watson 1992; Dengler and Nelson, 1999; Pyankov *et al.*, 2000; Edwards and Voznesenskaya, 2011). Additionally, K cells in  $C_4$  plants are commonly larger than the homologous cells of their more distant  $C_3$  relatives; however, size differences between K cells and the equivalent layer in closely related  $C_3$  relatives are often lacking (Hattersley *et al.*, 1982; Muhaidat *et al.* 2007; 2011; Christin *et al.* 2013). Chlorenchymatous M cells between veins are reduced in number in  $C_4$  relative to  $C_3$  leaves, such that only one layer of photosynthetic M cells surrounds the K cells, and there is extensive wall-to-wall contact between the K and M cells (Fig. 1; [Supplementary Figs S1, S2](#); Brown, 1977; Hattersley and Watson, 1992; Edwards and Voznesenskaya, 2011). This reduction in M cell layers minimizes the resistance to metabolite flux between the M and K cells (Bräutigam and Weber, 2011). In some Kranz types, an extra layer of cells lies between the M and K cells (Edwards and Voznesenskaya, 2011). The most common example of this occurs in grasses and sedges where an additional layer of cells with few chloroplasts separates M cells from mestome sheath cells where  $CO_2$  is concentrated ([Supplementary Fig. S2C](#); Hattersley and Watson, 1992; Soros and Dengler, 2001).

The many versions of the  $C_4$  Kranz syndrome are also associated with distinct ultrastructural changes that are essential for  $C_4$  function (Voznesenskaya and Gamaley, 1986; Hatch 1987; Hattersley and Watson, 1992; Dengler and Nelson, 1999; Edwards and Voznesenskaya, 2011). These include variation in organelle size, number, and position within the K cells (Dengler and Nelson, 1999; Voznesenskaya *et al.*, 1999, 2007, 2010; 2013; Koteyeva *et al.*, 2011; Muhaidat *et al.*, 2011; Sage *et al.*, 2011b; Bissinger *et al.*, 2014). Additionally, many  $C_4$  monocots contain suberin in the wall of the K cells, a feature that is absent from the eudicots (Hattersley and Browning, 1981; Edwards and Voznesenskaya, 2011; Mertz and Brutnell, 2014). Suberin slows diffusive efflux, thus

helping to trap  $CO_2$  in the K cells (Laetsch, 1974; Mertz and Brutnell, 2014). Kranz cells with suberized walls often have centrifugally positioned organelles, whereas in leaves lacking suberized walls, the chloroplasts typically occur along the inner, centripetal region of the K cell ([Supplementary Figs S1B–D](#); Hattersley and Watson 1992; Dengler and Nelson, 1999). The organelles of K cells are also altered to meet the different requirements of the three biochemical subtypes of  $C_4$  photosynthesis. For example, photosystem II is depleted in the K cell chloroplasts of the NADP-ME subtypes, but not in the K-cell chloroplasts of the NAD-ME subtypes (Hattersley and Watson 1992; Dengler and Nelson, 1999; Edwards and Voznesenskaya, 2011; Furbank, 2011). In the NAD-ME subtype, the decarboxylating enzyme occurs in the mitochondria, whereas in the NADP-ME subtype, it is in the chloroplast (Hatch, 1987). As a result, K-cell mitochondria in NAD-ME species tend to be larger, more numerous, and closely associated with chloroplasts compared with NADP-ME species (Dengler and Nelson, 1999; Voznesenskaya *et al.*, 2010; Koteyeva *et al.*, 2011; Khoshhravesh *et al.*, 2012; Oakley *et al.*, 2014). In the M cells,  $C_4$  plants produce about half the number of chloroplasts as their  $C_3$  relatives, and the  $C_4$  chloroplasts cover much less of the M cell periphery than in  $C_3$  plants (Stata *et al.*, 2014). This reduction in chloroplast number enhances  $CO_2$  access to the PEP carboxylation sites in the cytosol of the  $C_4$  M cell. Also, the cell walls between M and K cells are enriched in plasmodesmata, which increases the rate of metabolite exchange between the two cell types (Hattersley 1984; Evert *et al.* 1977; Botha, 1992; Bräutigam and Weber, 2011). In summary, when all features associated with Kranz anatomy are considered, it is apparent that it represents a highly sophisticated suite of structural adaptations that not only establish the necessary compartmentalization required by the  $C_4$  carbon concentrating mechanism (CCM), but also produces the subcellular intricacy needed for efficient  $C_4$  photosynthesis.

How Kranz anatomy evolved remains one of the great mysteries of plant biology, and has recently become a hot topic because of ongoing efforts to engineer  $C_4$  photosynthesis into  $C_3$  crops, and the recognition that  $C_4$  evolution is a major

event in the formation of the modern biosphere (Edwards *et al.*, 2010; Covshoff and Hibberd, 2012; Christin *et al.*, 2013; Slewinski, 2013). Biologists are now in a much better position to resolve the Kranz enigma, as new developmental models and genomic tools facilitate the linkage of traits with the underlying genetic control (Covshoff *et al.*, 2012, 2014; Williams *et al.*, 2013; Fouracre *et al.*, 2014). Long-standing concepts of C<sub>4</sub> evolution can also be examined using phylogenetically informed comparisons that include C<sub>3</sub>–C<sub>4</sub> intermediate species from multiple lineages (McKown and Dengler, 2007; Muhaidat *et al.*, 2011; Christin *et al.*, 2011, 2013; Khoshravesh *et al.*, 2012; Ocampo *et al.*, 2013; Sage *et al.*, 2013). Of particular value have been phylogenies with enough species coverage to identify close, sister taxa of C<sub>3</sub> and C<sub>4</sub> plants and numerous species with traits that are intermediate between the C<sub>3</sub> and C<sub>4</sub> conditions (McKown *et al.*, 2005; Sage *et al.*, 2007; Feodorova *et al.*, 2010; Christin *et al.*, 2011; Kadereit and Freitag, 2011; Roalson, 2011; Grass Phylogeny Working Group II, 2012; Khoshravesh *et al.*, 2012; Freitag and Kadereit, 2013; Ocampo *et al.*, 2013; Bissinger *et al.*, 2014). As a result, it has been possible to propose models of C<sub>4</sub> evolution that postulate, and then test, the importance of intermediate steps (Monson and Rawsthorne, 2000; Sage 2004; Sage *et al.*, 2012; Heckmann *et al.*, 2013; Williams *et al.*, 2013). A major aspect of these models has been the origin of Kranz anatomy.

In this review, we present a structure-function analysis addressing how Kranz anatomy may have evolved (see Fouracre *et al.*, 2014 for developmental perspectives of the issue). We begin by describing the conceptual models of C<sub>4</sub> evolution proposed by Monson and Rawsthorne (Monson *et al.*, 1984; Rawsthorne, 1992; Rawsthorne and Bauwe, 1998; Monson, 1999; Monson and Rawsthorne, 2000) as modified by Sage *et al.*, (Sage, 2001, 2004; Sage *et al.*, 2012). These models postulate a central role for glycine shuttling in the evolution of the C<sub>4</sub> pathway. We also discuss the importance of photorespiration and present a case that Kranz anatomy originated as a structure to enable the trapping and recycling of photorespired CO<sub>2</sub>. Photorespiration has been termed the “bridge to C<sub>4</sub> photosynthesis” because in dealing with its consequences, many of the structural features essential to C<sub>4</sub> photosynthesis first evolved (Bauwe, 2011). As part of this discussion, we examine recent papers evaluating the critical initial phases of C<sub>4</sub> evolution that occur in the C<sub>3</sub> relatives of C<sub>4</sub> clades (for example, Muhaidat *et al.*, 2011; Christin *et al.*, 2013; Sage *et al.*, 2013; Williams *et al.*, 2013). These close C<sub>3</sub> sisters exhibit changes in organelle size, number and location that are associated with changes in the size and shape of the bundle sheath cells, such that an incipient version of Kranz anatomy is apparent. The term “proto-Kranz” has been coined to describe this condition, which may represent the initial phase of C<sub>4</sub> evolution (Muhaidat *et al.*, 2011; Sage *et al.*, 2012; 2013).

Before proceeding, we define and justify our use of certain key terms to avoid confusion with earlier uses and to have a system that allows us to delineate evolutionary transitions in anatomical forms and photosynthetic physiologies. The term C<sub>2</sub> photosynthesis refers to a CCM that uses a

photorespiratory glycine shuttle to concentrate CO<sub>2</sub> into an inner, BS-like compartment from the M tissue. This physiology has commonly been called C<sub>3</sub>–C<sub>4</sub> intermediacy, but “C<sub>3</sub>–C<sub>4</sub> intermediate” is inappropriate as it equates one specific trait with an evolutionary process that is comprised of many transitional characteristics, not just the glycine shuttle. In addition, the glycine shuttle is found in many species having no relationship to C<sub>4</sub> clades, and thus are not technically C<sub>3</sub>–C<sub>4</sub> intermediates (Sage *et al.*, 2011a). Furthermore, “C<sub>2</sub>” refers to the number of carbon atoms in the glycine molecule that transports CO<sub>2</sub> into the inner compartment, in the same manner that “C<sub>4</sub>” refers to the four-carbon compound that transports CO<sub>2</sub> into the K cells. With respect to anatomical terminology, we restrict our definition of Kranz anatomy to those anatomical features where a wreath-like arrangement of M and BS-like cells enables a functioning CCM. This follows Haberlandt’s (1914) suggestion that the Kranz-type has a distinct functional adaptation. By this definition, C<sub>3</sub> taxa with enlarged BS cells that have been listed as having Kranz anatomy (see for example, Metcalfe and Chalk, 1979, pages 214–215) would not have it, whereas the anatomical specializations associated with the C<sub>4</sub> and C<sub>2</sub> CCMs would represent two versions of Kranz anatomy. For clarity, we refer to the pronounced wreath-like anatomy of C<sub>4</sub> species as “C<sub>4</sub>-Kranz”, and the simplified wreath-like anatomy of C<sub>2</sub> species as “C<sub>2</sub>-Kranz” (see Supplementary Fig. S2 for examples of each). “Sub-Kranz” might be a logical alternative to C<sub>2</sub>-Kranz, but we feel this is inadequate as it implies the anatomy of C<sub>2</sub> species is an incomplete version of C<sub>4</sub>-Kranz, rather than a structural adaptation in its own right that enables efficient function of the C<sub>2</sub> CCM. Sub-Kranz also does not connect the anatomy to the specific physiological adaptation, and can be confused with proto-Kranz, the term we use for anatomical changes in C<sub>3</sub> species that precede C<sub>2</sub>-Kranz. Finally, we use the term BS (bundle sheath) cells in place of K cells because we repeatedly refer to the evolutionary transition from BS-like cells lacking a CCM to Kranz cells with a CCM, and the distinction between the two may not always be clear.

## The Monson family of models for C<sub>4</sub> evolution

The high number of C<sub>4</sub> origins allow for the testing of evolutionary hypotheses using the methods of comparative biology, where each lineage represents an independent observation of one evolutionary transition (Ackerly, 1999; Christin *et al.*, 2013). Using such approaches, the evidence from the many C<sub>4</sub> lineages consistently supports gradual models of C<sub>4</sub> origin, with a critical intermediate role for a glycine shuttle that concentrates photorespired CO<sub>2</sub> into a BS-like compartment (Fig. 2; Monson and Rawsthorne, 2000; Sage *et al.*, 2012; Williams *et al.*, 2013). The glycine shuttle CCM was first proposed by Monson *et al.* (1984) to explain the photosynthetic physiology of the C<sub>3</sub>–C<sub>4</sub> intermediate species known at that time (Rawsthorne *et al.*, 1988, Rawsthorne, 1992 and Monson 1999 for follow-ups). Glycine shuttling has since been identified in over 50 C<sub>2</sub> species from 20 or so evolutionary lineages

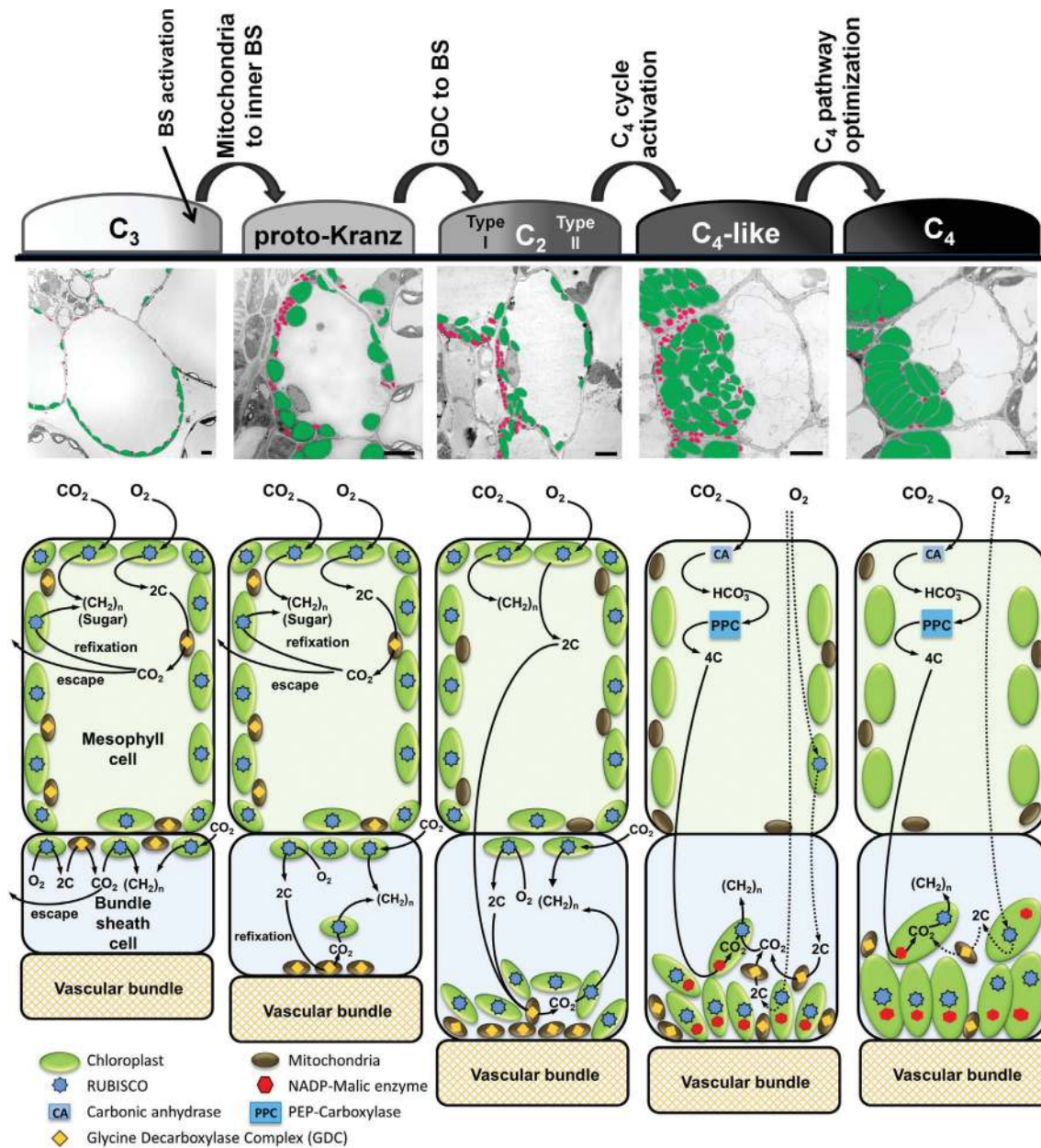


**Fig. 2.** A diagram illustrating the evolutionary progression from C<sub>3</sub> to C<sub>4</sub> photosynthesis via three distinct phases termed proto-Kranz, C<sub>2</sub> photosynthesis (C<sub>2</sub>), and C<sub>4</sub>-like photosynthesis. Arrows indicate the major changes between the phases. Note that bundle-sheath (BS) activation occurs within the C<sub>3</sub> group as indicated by the transition to grey shading; this refers to the increase in photosynthetic activity in the BS following an increase in organelle numbers and BS cell size. Immediately below are false-colour transmission electron micrographs showing chloroplasts (green) and mitochondria (red) for five *Flaveria* species that are classified as C<sub>3</sub>, proto-Kranz, C<sub>2</sub>, C<sub>4</sub>-like, and C<sub>4</sub> plants. The bottom row illustrates carbon flow in the mesophyll (M) and BS tissues of the C<sub>3</sub> and proto-Kranz types, and between the M and BS in the C<sub>2</sub>, C<sub>4</sub>-like, and C<sub>4</sub> types. 2C indicates the two-carbon photorespiratory metabolite glycine; (CH<sub>2</sub>)<sub>n</sub> refers to leaf carbohydrate. Type I refers to C<sub>2</sub> photosynthesis and little associated C<sub>4</sub> cycle; Type II refers to C<sub>2</sub> photosynthesis with a modest C<sub>4</sub> cycle. Developed from Edwards and Ku, 1987; Moore et al., 1987b; Ku et al., 1991; Monson and Rawsthorne, 2000; Muhaidat et al., 2011; and Sage et al., 2012. Bars=5 μm. Explanation: *Flaveria cronquistii*, *F. robusta*, and *F. linearis* demonstrate the development of BS from an expanded, activated C<sub>3</sub> condition to the mitochondria-enriched BS of the proto-Kranz and C<sub>2</sub> conditions. The main difference between these proto-Kranz and C<sub>2</sub> species is the high expression of glycine decarboxylase (GDC) in the M cells of *F. robusta*, compared with low expression of GDC in the M cells of *F. linearis* (not shown). The shift from the C<sub>2</sub>-Kranz to C<sub>4</sub>-Kranz forms is accompanied by an enlargement of BS chloroplasts and a reduction in BS mitochondria in this C<sub>4</sub> NADP-ME lineage. With respect to carbon flow, the M and BS cells in C<sub>3</sub> plants operate independently, with each assimilating O<sub>2</sub> and CO<sub>2</sub> and processing the fixation products to either CO<sub>2</sub> (via glycine decarboxylase, GDC, in the mitochondria) or carbohydrate (via photosynthesis). The CO<sub>2</sub> produced by GDC can then either escape the cell or be refixed. In proto-Kranz species, the movement of mitochondria and a few chloroplasts to the inner wall of the BS cells forces the glycine formed by outer chloroplasts to migrate to the inner BS for decarboxylation, with the released CO<sub>2</sub> accumulating and increasing Rubisco efficiency. This represents a single-celled, BS-specific glycine shuttle. In Type I C<sub>2</sub> species, GDC is largely restricted to BS cells, so that photorespiratory glycine diffuses to GDC located in centripetal mitochondria. The released CO<sub>2</sub> accumulates and enhances Rubisco activity in the numerous chloroplasts in the inner BS. This is the two-celled photorespiratory glycine shuttle that boosts BS CO<sub>2</sub> levels. In the C<sub>4</sub>-like pattern, a strong C<sub>4</sub> biochemical cycle moves 4C organic acids into the BS, whereas a weak two-celled glycine shuttle remains to process any glycine produced by the residual Rubisco in the M cells. In most C<sub>4</sub> leaves, the only way to move carbon from the M to BS cells is via the C<sub>4</sub> metabolic cycle involving PEP carboxylation.

**Table 1.** The classification of the known C<sub>3</sub>–C<sub>4</sub> intermediate species into proto-Kranz, C<sub>2</sub> photosynthesis, and C<sub>4</sub>-like photosynthesis

A clade of closely related C<sub>4</sub> species is also listed, if relevant. A listing of C<sub>2</sub> alone indicates the strength of C<sub>4</sub> metabolism is unknown. Compiled from Table 2 of Sage *et al.*, 2011a; Table V in Sage *et al.*, 1999 and references listed.

| C <sub>2</sub> clade | Species                             | Photosynthetic category                                     | Closely related C <sub>4</sub> clade        | Reference   |
|----------------------|-------------------------------------|---|---|---|
| Amaranthaceae        | <i>Alternanthera ficoides</i>       | Type I C <sub>2</sub>                                       | <i>Alternanthera</i>                        | Rajendrudu <i>et al.</i> , 1986   |
|                      | <i>A. tenella</i>                   | Type I C <sub>2</sub>                                       | <i>Alternanthera</i>                        | as with <i>A. ficoides</i>  |
| Asteraceae           | <i>Flaveria pringlei</i>            | Proto-Kranz   | <i>Flaveria</i> A, B                        | Edwards & Ku, 1987; Ku <i>et al.</i> 1991; McKown <i>et al.</i> , 2005; Vogan and Sage, 2011; Sage <i>et al.</i> , 2013 |
|                      | <i>F. robusta</i>                   | Proto-Kranz   | <i>Flaveria</i> A, B                        | as with <i>F. pringlei</i>  |
|                      | <i>F. sonorensis</i>                | Type I C <sub>2</sub>                                       | <i>Flaveria</i> A, B                        | as with <i>F. pringlei</i>  |
|                      | <i>F. ramosissima</i>               | Type II C <sub>2</sub>                                      | <i>Flaveria</i> A                           | as with <i>F. pringlei</i>  |
|                      | <i>F. palmeri</i>                   | C <sub>4</sub> -like  | <i>Flaveria</i> A                           | as with <i>F. pringlei</i>  |
|                      | <i>F. vaginata</i>                  | C <sub>4</sub> -like  | <i>Flaveria</i> A                           | as with <i>F. pringlei</i>  |
|                      | <i>F. angustifolia</i>              | Type I C <sub>2</sub>                                       | <i>Flaveria</i> B                           | as with <i>F. pringlei</i>  |
|                      | <i>F. anomala</i>                   | Type II C <sub>2</sub>                                      | <i>Flaveria</i> B                           | Edwards and Ku, 1987; Ku <i>et al.</i> , 1991   |
|                      | <i>F. chloraefolia</i>              | Type I C <sub>2</sub>                                       | <i>Flaveria</i> B                           | as with <i>F. pringlei</i>  |
|                      | <i>F. pubescens</i>                 | Type II C <sub>2</sub>                                      | <i>Flaveria</i> B                           | Edwards and Ku, 1987; Ku <i>et al.</i> , 1991   |
|                      | <i>F. linearis</i>                  | Type II C <sub>2</sub>                                      | <i>Flaveria</i> B                           | as with <i>F. pringlei</i>  |
|                      | <i>F. floridana</i>                 | Type II C <sub>2</sub>                                      | <i>Flaveria</i> B                           | as with <i>F. pringlei</i>  |
|                      | <i>F. oppositifolia</i>             | C <sub>2</sub>  | <i>Flaveria</i> B                           | as with <i>F. pringlei</i>  |
|                      | <i>F. brownii</i>                   | C <sub>4</sub> -like  | <i>Flaveria</i> B                           | as with <i>F. pringlei</i>  |
| Parthenium           | <i>P. hysterophorus</i>             | Type I C <sub>2</sub>                                       | None  | Edwards and Ku, 1987; Moore <i>et al.</i> , 1987a   |
| Boraginaceae         | <i>Heliotropium karwinskyi</i>      | Proto-Kranz   | Mexican C <sub>4</sub> clade                | Frohlich, 1978; Vogan <i>et al.</i> , 2007; Muhaidat <i>et al.</i> , 2011   |
|                      | <i>H. procumbens</i>                | Proto-Kranz   | None  | as with <i>H. karwinskyi</i>  |
|                      | <i>H. convolvulaceum</i>            | Type I C <sub>2</sub>                                       | Mexican C <sub>4</sub> clade                | as with <i>H. karwinskyi</i>  |
|                      | <i>H. racemosum</i>                 | Type I C <sub>2</sub>                                       | Mexican C <sub>4</sub> clade                | as with <i>H. karwinskyi</i>  |
|                      | <i>H. greggii</i>                   | Type I C <sub>2</sub>                                       | S. American C <sub>4</sub> clade            | as with <i>H. karwinskyi</i>  |
|                      | <i>H. lagoense</i>                  | C <sub>2</sub>  | S. American C <sub>4</sub> clade            | as with <i>H. karwinskyi</i>  |
| Brassicaceae         | <i>Diplotaxis tenuifolia</i>        | Type I C <sub>2</sub>                                       | None  | Apel <i>et al.</i> , 1997   |
|                      | <i>Diplotaxis erucoides</i>         | C <sub>2</sub>  | None  | Apel <i>et al.</i> , 1997   |
|                      | <i>Diplotaxis muralis</i>           | C <sub>2</sub>  | None  | Apel <i>et al.</i> , 1997   |
|                      | <i>Moricandia arvensis</i>          | Type I C <sub>2</sub>                                       | None  | Holiday and Chollet, 1984   |
|                      | <i>M. nitens</i>                    | C <sub>2</sub>  | None  | as with <i>M. arvensis</i>  |
|                      | <i>M. sinaica</i>                   | C <sub>2</sub>  | None  | as with <i>M. arvensis</i>  |
|                      | <i>M. spinosa</i>                   | C <sub>2</sub>  | None  | as with <i>M. arvensis</i>  |
|                      | <i>M. suffruticosa</i>              | C <sub>2</sub>  | None  | as with <i>M. arvensis</i>  |
| Chenopodiaceae       | <i>Sedobassia sedoides</i>          | C <sub>2</sub>  | Camphorosmae                                | Freitag and Kadereit, 2013; this study  |
|                      | <i>Salsola montana</i>              | Proto-Kranz   | None  | Voznesenskaya <i>et al.</i> , 2013  |
|                      | <i>S. arbusculiformis</i>           | Type I C <sub>2</sub>                                       | None  | Voznesenskaya <i>et al.</i> , 2001, 2013  |
|                      | <i>S. divaricata</i>                | Type I C <sub>2</sub>                                       | None  | Voznesenskaya <i>et al.</i> , 2013  |
| Cleomaceae           | <i>Cleome paradoxa</i>              | Type I C <sub>2</sub>                                       | <i>Cleome angustifolia</i>                  | Voznesenskaya <i>et al.</i> , 2007; Feodorova <i>et al.</i> , 2010  |
| Euphorbiaceae        | <i>Euphorbia acuta</i>              | Type I C <sub>2</sub>                                       | <i>Euphorbia</i> subgenus <i>Chamaesyce</i> | Sage <i>et al.</i> 2011b; Yang and Berry, 2011  |
|                      | <i>E. johnstonii</i>                | C <sub>2</sub>  | <i>Euphorbia</i> subgenus <i>Chamaesyce</i> | as with <i>E. acuta</i>   |
| Molluginaceae        | <i>Mollugo nudicaulis</i>           | Type I C <sub>2</sub>                                       | <i>Mollugo cerviana</i>                     | Christin <i>et al.</i> , 2011   |
|                      | <i>M. verticillata</i>              | Type II C <sub>2</sub>                                      | <i>Mollugo cerviana</i>                     | Edwards and Ku, 1987; Christin <i>et al.</i> , 2011   |
| Nyctaginaceae        | <i>Bouganvillea</i> cv. Mary Palmer | C <sub>2</sub>  | None  | Sabale and Bhosale, 1984  |
| Portulacaceae        | <i>Portulaca cryptopetala</i>       | Type I C <sub>2</sub>                                       | <i>Portulaca</i>                            | Voznesenskaya <i>et al.</i> , 2010; Ocampo <i>et al.</i> , 2013   |
| Scrophulariaceae     | <i>Anticharis</i> spp.              | Multiple C <sub>2</sub> candidates from herbarium specimens | <i>Anticharis</i>                           | Khoshraveh <i>et al.</i> , 2012   |
| Cyperaceae           | <i>Eleocharis</i> spp               | Multiple C <sub>2</sub> candidates                          | Unknown                                     | Roalson <i>et al.</i> , 2010  |
| Hydrocharitaceae     | <i>Vallisneria spiralis</i>         | Uncertain   | Unknown                                     | Keeley, 1990  |

Table 1. Continued

| C <sub>2</sub> clade | Species                    | Photosynthetic category | Closely related C <sub>4</sub> clade       | Reference   |
|----------------------|----------------------------|-------------------------|--|---|
| Poaceae              | <i>Homolepis aturensis</i> | C <sub>2</sub> anatomy  | <i>Mesosetum</i> and/or <i>Arthropogon</i> | Grass Phylogeny Working Group II, 2012; Christin et al., 2013       |
|                      | <i>Neurachne minor</i>     | Type I C <sub>2</sub>   | <i>Paraneurachne</i>                       | Hattersley et al., 1986; Moore et al., 1989; Christin et al., 2012  |
|                      | <i>Panicum hylaeicum</i>   | Proto-Kranz             | None                                       | Holaday and Black, 1981; Brown et al., 1983; Aliscioni et al., 2003 |
|                      | <i>Steinchisma laxa</i>    | Proto-Kranz             | None                                       | as with <i>P. hylaeicum</i>   |
|                      | <i>S. cuprea</i>           | C <sub>2</sub>          | None                                       | as with <i>P. hylaeicum</i>   |
|                      | <i>S. decipiens</i>        | C <sub>2</sub>          | None                                       | as with <i>P. hylaeicum</i>   |
|                      | <i>S. exiguiflora</i>      | C <sub>2</sub>          | None                                       | as with <i>P. hylaeicum</i>   |
|                      | <i>S. hians</i>            | Type I C <sub>2</sub>   | None                                       | Edwards and Ku, 1987  |
|                      | <i>S. spathellosa</i>      | C <sub>2</sub>          | None                                       | as with <i>P. hylaeicum</i>   |
|                      | <i>S. stenophylla</i>      | C <sub>2</sub>          | None                                       | as with <i>P. hylaeicum</i>   |

(Table 1). Monson, Rawsthorne, and co-workers originally proposed a series of conceptual models for the evolutionary progression from C<sub>3</sub> to C<sub>4</sub> species, based on the variation observed in C<sub>2</sub> species of *Alternanthera*, *Flaveria*, *Mollugo*, *Moricandia*, *Neurachne*, and *Panicum/Steinchisma* (Monson and Moore, 1989; Monson, 1989, 1999; Rawsthorne, 1992; Rawsthorne and Bauwe, 1998; Monson and Rawsthorne, 2000). In recent years, numerous groups have built upon these conceptual models as data has become available from newly described C<sub>3</sub> to C<sub>4</sub> lineages (Sage, 2004; McKown and Dengler, 2007; Bauwe, 2011; Sage et al., 2012). All of these models propose the glycine shuttle-type CCM as the key intermediate step between the C<sub>3</sub> and C<sub>4</sub> conditions. For this reason, we classify these as the Monson family of C<sub>4</sub> evolutionary models.

Figure 2 presents a schematic of C<sub>4</sub> evolution that follows from Monson and Rawsthorne (2000) and a recent iteration in Sage et al. (2012). For simplicity, we present the model as a flow scheme that documents the transition from C<sub>3</sub> to C<sub>4</sub> as moving through a series of intermediate phases; these correspond to known physiological states in existing lineages, and their order is consistent with phylogenetic patterns observed in those lineages. Three distinct intermediate phases are delineated, which we term (i) proto-Kranz, (ii) C<sub>2</sub> photosynthesis or the photorespiratory glycine shuttle, and (iii) C<sub>4</sub>-like photosynthesis (Fig. 2). Four key transitions are noted. The first is BS activation, which occurs within the C<sub>3</sub> condition. Activation of the BS occurs when the BS cells engage in substantial photosynthetic activity owing to increases in their size and chloroplast number (Gowik and Westhoff, 2011; Sage et al., 2013). *Flaveria cronquistii* is representative of a C<sub>3</sub> plant with an activated BS (Fig. 2). The key transitions following BS activation are the shift in the location of mitochondria from the outer to the inner BS, the localization of glycine decarboxylase (GDC) to the BS cells, and the activation of the C<sub>4</sub> metabolic pump (Fig. 2). Figure 2 also indicates the transition from a Type I to Type II condition within the C<sub>2</sub> phase. In the Type I subphase, the glycine shuttle alone concentrates CO<sub>2</sub> in the BS, whereas in the Type II subphase, the glycine shuttle is accompanied by modest C<sub>4</sub> metabolism.

This follows the delineation of Type I and II C<sub>3</sub>–C<sub>4</sub> intermediates by Edwards and Ku (1987).

The scheme in Figure 2 is conceptual and qualitative in nature. In the past year, two independent efforts have developed more complex, quantifiable models that use an adaptive landscape approach to analyse the details of the C<sub>4</sub> evolutionary process (Heckmann et al. 2013; Williams et al., 2013). Heckmann et al. (2013) use a theoretical photosynthesis model (von Caemmerer, 2000) to quantify a fitness landscape across which evolutionary trajectories are modelled for the following six parameters: (i) fraction of Rubisco in the M tissue, (ii) Rubisco turnover capacity, (iii) fraction of GDC activity in the BS, (iv) C<sub>4</sub> cycle activity, (v) the  $K_m$  of PEP carboxylase for bicarbonate, and (vi) the conductance of the BS for gases (Heckmann et al., 2013). In the model, these six traits were randomly altered between C<sub>3</sub> and C<sub>4</sub> values. If fitness increased following the single trait change, the trait could be fixed, and then built upon if a subsequent trait change increased fitness. This iterative process continued until the modelled phenotypes arrived at the C<sub>4</sub> condition for all traits. With respect to Kranz evolution, Heckmann et al. (2013) present two important findings. First, the formation of a glycine shuttle (and the C<sub>2</sub>-Kranz anatomy that enables glycine shuttling) is the critical early phase in the biochemical evolution of C<sub>4</sub> photosynthesis. This theoretical result independently supports the empirical findings summarized in Fig. 2. Second, an extensive series of changes representing the biochemical evolution of the C<sub>4</sub> pathway largely corresponds to the “C<sub>4</sub> cycle activation” and “optimization” steps in Fig. 2 and thus would also correspond to the transition from C<sub>2</sub>-Kranz to C<sub>4</sub>-Kranz. Heckmann et al. (2013) did not directly model any specific anatomical change, but did include a number of parameters whose trait values would encompass anatomical changes. Of these, reduction in the BS conductance to CO<sub>2</sub> efflux is modelled to occur late, after activation of the C<sub>4</sub> biochemical cycle. Reduced BS conductance would largely reflect structural evolution, for example through thickening of the outer BS wall (von Caemmerer and Furbank, 2003).

In Williams et al. (2013), a meta-analysis of 43 studies of C<sub>3</sub>–C<sub>4</sub> intermediates was used to quantify 16 biochemical,

anatomical, and cellular traits to parameterize a phenotypic landscape. The evolution of C<sub>4</sub> photosynthesis across this landscape was then modelled as a transition network, and a time-ordered acquisition of traits was predicted based on the series of networks that were most compatible with the meta-analysis. For eudicots, the trait appearance predicted by the model was consistent with the qualitative scheme depicted in Fig. 2, in that changes in vein density, BS cell size, and GDC specificity occur early in C<sub>4</sub> evolution to establish the proto-Kranz and C<sub>2</sub>-like conditions. Most of the biochemical changes were modelled to occur later, in what would correspond to the C<sub>4</sub> cycle activation and optimization phases of Fig. 2. The order of trait appearance in monocots differed, but Williams *et al.* (2013) had a limited set of C<sub>3</sub>–C<sub>4</sub> intermediate grasses to parameterize the model, and so these predictions are tentative.

At this point, we evaluate the empirical and theoretical evidence for the structural changes that are thought to have occurred during C<sub>4</sub> evolution. We begin by discussing the anatomical traits in C<sub>3</sub> plants that may have enabled the initiation of C<sub>4</sub> evolution.

### Setting the stage—the rise of anatomical enablers in the C<sub>3</sub> flora

Although C<sub>4</sub> photosynthesis evolved in taxonomic groups scattered throughout the angiosperm phylogeny, it tends to cluster in three major clades: the grasses (22–24 independent origins; GWPGII, 2012), the Caryophyllales (23 independent origins; Sage *et al.*, 2011a), and the sedges (six independent origins; Besnard *et al.*, 2009). As striking as this clustering is, the complete absence of C<sub>4</sub> photosynthesis in diverse and adaptable lineages such as the large orders containing the legumes, roses, lilies, and orchids is also noteworthy. Many of these groups are common in the same habits as C<sub>4</sub> species and numerous genera within these orders have evolved CAM, indicating photosynthetic flexibility (Smith and Winter, 1996; Sage, 2002). These patterns suggest there may be a series of predisposing traits that facilitate C<sub>4</sub> evolution in some taxa, whereas the lack of such traits may preclude C<sub>4</sub> evolution in other taxa. Preconditioning traits in C<sub>3</sub> species that may promote diversification of Kranz tissues include high vein density and enlarged BS cells (Sage, 2004; Muhaidat *et al.*, 2011; Sage *et al.*, 2012; Christin *et al.*, 2013; Griffiths *et al.*, 2013).

The identification of most lineages of C<sub>4</sub> photosynthesis has allowed for an evaluation of the environmental conditions where the C<sub>4</sub> pathway arose. In the eudicots, centres of origin have been postulated for 35 of the 36 known clades and it is possible to identify centres of origin for a handful of grass lineages (Sage *et al.*, 2011a; Christin *et al.*, 2012). The centres of origin generally correspond to hot, monsoon-affected regions, or non-monsoon areas where there is sufficient soil moisture to support summer photosynthesis. Most areas also correspond to where periodic aridity and low atmospheric humidity promote recurring episodes of water and/or salinity stress. Salinity seems to be a particularly important driver for C<sub>4</sub> evolution in the Chenopodiaceae lines of central Asia

(Djamali *et al.*, 2012; Kadereit *et al.*, 2012; Sage *et al.*, 2011a). These conditions maximize the potential for photorespiration, but also create high evapotranspiration potentials that could lead to hydraulic crisis in leaves should the stomata remain open, or restrict carbon gain should stomata close to conserve water (Osborne and Sack, 2012; Sage, 2013). The key role of the monsoons is that they supply moisture during the summer season, creating moist growing conditions in what is often a hot, low humidity setting (Sage *et al.*, 2012). In these conditions, high vein density in leaves is proposed to be adaptive because it can deliver water fast enough to maintain tissue water status and prevent premature stomatal closure (Sage, 2001, 2004; Osborne and Sack, 2012). Consistently, C<sub>3</sub> species from hot, semi-arid regions often have greater vein density (Roth-Nebelsick *et al.*, 2001). High vein density seems to be particularly common in the C<sub>3</sub> sister clades of many C<sub>4</sub> lineages (Osborne and Sack, 2012; Sage *et al.*, 2012; Griffiths *et al.*, 2013). For example, vein density approaches or equals C<sub>4</sub> values in C<sub>3</sub> sister groups of *Anticharis* (Khoshnavesh *et al.*, 2012), *Cleome* (Marshall *et al.*, 2007; Voznesenskaya *et al.*, 2007), *Heliotropium* (Muhaidat *et al.*, 2011), *Euphorbia* (Sage *et al.*, 2011b), *Mollugo* (Christin *et al.*, 2011), and *Salsola* (Voznesenskaya *et al.*, 2013). In a survey of species from 54 related C<sub>3</sub> and C<sub>4</sub> species from 13 eudicot families, no statistical difference was observed in vein density between the means of the C<sub>3</sub> and C<sub>4</sub> groups (Muhaidat *et al.*, 2007). Many C<sub>3</sub> grasses that are sister to the C<sub>4</sub> grass clades also have reduced interveinal distance, reflecting elevated vein density (Christin *et al.*, 2013).

Large BS size is also considered an important anatomical feature that may be more common in dry environments. Larger BS cells are posited to improve hydraulic capacitance in leaves and thus buffer surges in transpiration caused by wind gusts (Sage, 2004; Griffiths *et al.*, 2013). As with increased vein density, increased BS size is commonly found in the C<sub>3</sub> relatives of C<sub>4</sub> clades. Most of the C<sub>3</sub> sister groups of C<sub>4</sub> lineages in the PACMAD clade of grasses have increased BS volumes relative to M volumes (Brown *et al.*, 1983; Christin *et al.*, 2012, 2013; Griffiths *et al.*, 2013). In *Flaveria* and related genera, enlarged BS cells are present in the C<sub>3</sub> species *F. cronquistii* (Fig. 2) and its sister genus *Sartwellia* (McKown and Dengler, 2007; Sage *et al.*, 2013). Large BS cells are also present in a C<sub>3</sub> *Euphorbia* that is sister to the C<sub>2</sub> clade in *Euphorbia* section *acutae* (Sage *et al.*, 2011b). In *Heliotropium*, the closest C<sub>3</sub> relatives to the C<sub>4</sub> clades have enlarged BS cells relative to less-related C<sub>3</sub> species (Muhaidat *et al.*, 2011). In *Atriplex*, the C<sub>3</sub> and C<sub>4</sub> species that are related enough to form fertile hybrids also have similar BS cell size (Oakley *et al.*, 2014). In the Muhaidat *et al.* (2007) comparison of 54 C<sub>3</sub> and C<sub>4</sub> species from 13 dicot families, C<sub>3</sub> species had on average smaller BS cells; however, the BS cell size of many C<sub>3</sub> taxa overlapped with that of their C<sub>4</sub> relatives.

Understanding how increased vein density and BS size facilitates Kranz evolution requires close examination of BS ultrastructure and morphology. In C<sub>3</sub> species that branch in sister positions to C<sub>2</sub> or C<sub>4</sub> species in the *Anticharis*, *Cleome*, *Euphorbia*, *Flaveria*, and *Heliotropium* phylogenies, enlarged BS cells protrude into the mesophyll, forming

spongy-parenchyma-like cells (Fig. 2; Marshall *et al.*, 2007 for *Cleome*; Muhaidat *et al.*, 2011 for *Heliotropium*; Sage *et al.*, 2011b for *Euphorbia*; Sage *et al.*, 2013 for *Flaveria*). The BS cell protrusions enhance exposure to the intercellular air space (IAS), thereby allowing many chloroplasts to be positioned along the perimeter of the BS cell that faces the IAS, as shown for *F. cronquistii* (Fig. 2). Notably, as observed in C<sub>3</sub> species of *Euphorbia*, *Flaveria* and *Heliotropium*, the BS chloroplasts facing the IAS occur near mitochondria, in an identical arrangement as that in M cells (Muhaidat *et al.*, 2011; Sage *et al.*, 2011b; Sage *et al.*, 2013). This close arrangement of mitochondria and chloroplasts facilitates rapid flux of metabolites between the two organelles during photorespiratory metabolism (Busch *et al.*, 2013). Enhancement of chloroplast numbers against the IAS wall of the BS cells is strong evidence that the BS has become heavily engaged in photosynthetic carbon assimilation, or following the terminology of Gowik and Westhoff (2011), the BS has become “activated”. Photosynthetic activation of the BS is suggested to compensate for the loss of M cell volume as veins become more abundant in the leaf and BS cells expand (Sage *et al.*, 2012; 2013). Its significance for C<sub>4</sub> evolution is that the BS cells begin to generate large amounts of photorespiratory CO<sub>2</sub> in hot climates of low atmospheric CO<sub>2</sub>. This formation of photorespired CO<sub>2</sub> represents an opportunity for improved carbon gain if the CO<sub>2</sub> production can be localized to a BS region where it can be trapped and refixed. As discussed next, the evolution of CO<sub>2</sub> trapping and refixation is proposed to give rise to the proto-Kranz condition and the first definitive step in C<sub>4</sub> evolution.

## The proto-Kranz condition

As first described for two *Heliotropium* species (*H. procumbens* and *H. karwinskyi*), the proto-Kranz condition consists of enlarged BS cells relative to a typical C<sub>3</sub> *Heliotropium* species, and the BS tissue is more circular in outline than in the uneven edge produced by enlarged, spongy-like BS cells of the sister C<sub>3</sub> species *H. tenellum* (Muhaidat *et al.*, 2011). The more uniform BS outline in the proto-Kranz species is associated with a reduction in the exposure of the BS cells to the IAS. Mitochondria in the BS are larger in the two proto-Kranz *Heliotropium* species, and in *H. procumbens*, there are double the number of mitochondria relative to the C<sub>3</sub> sister species. Of particular note is the localization of 82–97% of the mitochondria to the inner wall of the BS in *H. karwinskyi* and *H. procumbens*, respectively (Muhaidat *et al.*, 2011). In *H. tenellum*, by contrast, mitochondria are spread around the cell periphery. The localization of mitochondria to the centripetal pole of the BS cells produced a distinct band of immunolocalization stain for glycine decarboxylase (GDC) along the inner edge of the BS, in a pattern that is similar to, though less intense, than that of C<sub>2</sub> species (Fig. 3A–C). Unlike the C<sub>2</sub> species, GDC is still common in the M cells of proto-Kranz species.

Muhaidat *et al.* (2011) drew attention to proto-Kranz anatomy described by Brown *et al.*, (1983) in the *Steinchisma*

clade of grasses. *Steinchisma laxa* (formerly *Panicum laxum*) is sister to a C<sub>2</sub> clade of *Steinchisma*, whereas *Panicum hylaecium* is close to the *Steinchisma* clade (Aliscioni *et al.*, 2003). Both species have C<sub>3</sub> gas exchange characteristics and BS cells that are of similar size as the C<sub>2</sub> species of *Steinchisma*; however, the BS cells exhibit over 3-fold more BS chloroplasts, and *S. laxa* has 8-fold more mitochondria than a typical C<sub>3</sub> *Panicum* species (Morgan and Brown, 1980; Brown *et al.*, 1983). Nearly all of the BS mitochondria in *S. laxa* are arrayed along the inner BS wall where it contacts the vascular tissue. In *S. laxa*, there is also a layer of chloroplasts adjacent to the layer of mitochondria as is widely observed in C<sub>2</sub> species (Brown *et al.*, 1983). Curiously, in both *S. laxa* and *P. hylaecium*, many of the chloroplasts encapsulate the mitochondria (Brown *et al.* 1983), a feature that has been linked to increased refixation of photorespired CO<sub>2</sub> (Busch *et al.*, 2013).

In addition to *Heliotropium* and *Panicum/Steinchisma*, the proto-Kranz condition has recently been recognized in *Salsola montana* of the Chenopodiaceae (Voznesenskaya *et al.*, 2013) and two C<sub>3</sub> *Flaveria* species in the sunflower family, *F. pringlei* and *F. robusta* (Sage *et al.*, 2013). In *S. montana*, the leaf has a “sympegmoid” anatomy formed by concentric layers of mesophyll cells surrounding a central core of succulent water storage tissue and veins (Voznesenskaya *et al.*, 2013). Bundle-sheath cells occur beside the veins at the edge of the water storage tissue. Mitochondria in *S. montana* are localized to the wall against the vascular tissue in these BS cells, leading to its designation as a proto-Kranz species (Voznesenskaya *et al.*, 2013).

In *Flaveria*, detailed examination of the species branching at the basal nodes of the phylogeny has identified two species previously categorized as C<sub>3</sub> (*F. pringlei* and *F. robusta*) as having proto-Kranz features similar to those observed in *Heliotropium* (Sage *et al.*, 2013). In the *Flaveria* phylogeny, *F. pringlei* and *F. robusta* branch at nodes between the C<sub>3</sub> *F. cronquistii* node and the nodes for the C<sub>2</sub> species *F. sonorensis* and *F. angustifolia* (McKown *et al.*, 2005). In the basal branching *F. cronquistii* and its sister species *Sartwellia flaveriinae*, BS cells are enlarged with elongated spongy-like protrusions, whereas in *F. pringlei* and *F. robusta*, the BS cells have coalesced into a more even edged-sheath with low exposure to the IAS (Sage *et al.*, 2013). Bundle-sheath cells in *F. pringlei* and *F. robusta* are enlarged compared with a typical C<sub>3</sub> species such as sunflower but are actually smaller than their immediate C<sub>3</sub> sister species that branch lower in the phylogeny (McKown and Dengler, 2007; Sage *et al.*, 2013). This is due to the loss of the lobing observed in the expansive BS cells of *F. cronquistii*. In *F. pringlei* and *F. robusta*, organelle numbers are enhanced, and 75% or more of the BS mitochondria are centripetally located, which approximates the mitochondria distribution in the BS of C<sub>2</sub> species (Fig. 2; Sage *et al.*, 2013). Both *F. pringlei* and *F. robusta* have a distinct band of GDC stain along the inner BS wall, yet both also express GDC in the M mitochondria (Fig. 3D–F). This GDC distribution is similar to what has been reported for the proto-Kranz species in the genus *Heliotropium* (Fig. 3; Muhaidat *et al.*, 2011). In *F. robusta*, numerous chloroplasts also occur beside the



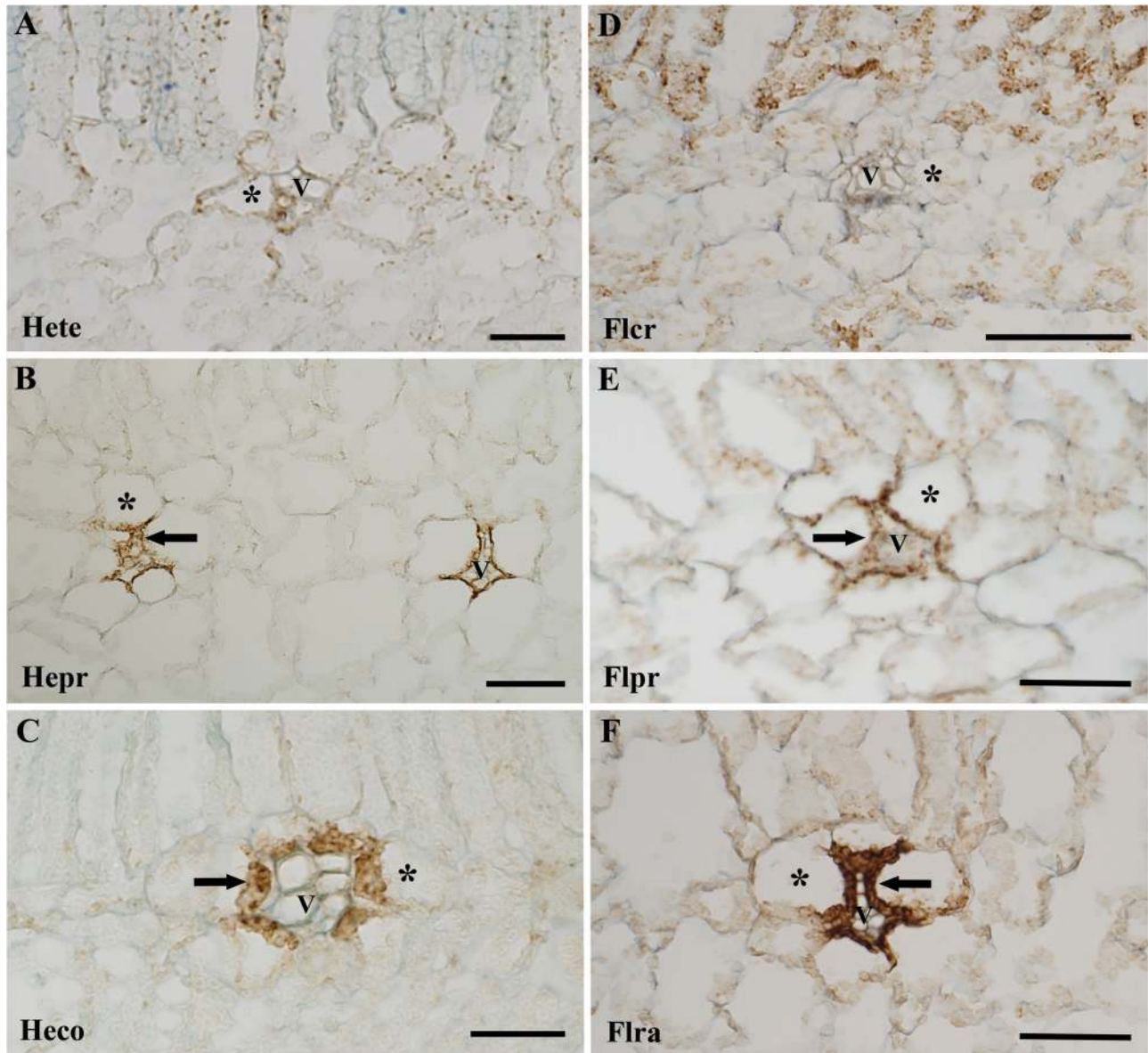


**Fig. 3.** *In situ* immunolocalization of GDC p-protein subunit in the leaves of C<sub>3</sub> (A, D), proto-Kranz (B, E), and C<sub>2</sub> (C, F) species in the genus *Heliotropium* (A–C) and *Flaveria* (D, E). Hete, *H. tenellum*; Hepr, *H. procumbens*; Heco, *H. convovulaceum*; Flcr, *F. cronquistii*; Flro, *F. robusta*; Flra, *F. ramosissima*. Brown stain indicates the presence of GDC. Asterisks indicate bundle sheath cells and arrows point out bundle sheath mitochondria. V indicates vascular tissue. Bars=50  $\mu\text{m}$ .

centripetal BS mitochondria in a pattern similar to that of many C<sub>2</sub> species (Figs 2, 4; Sage *et al.*, 2013).

The observation that C<sub>3</sub> proto-Kranz species are closely related to C<sub>2</sub> species in four independent lineages supports a hypothesis that the proto-Kranz condition is an early phase of C<sub>2</sub> evolution, and in turn, C<sub>4</sub> evolution. If this is the case, it is logical to assume there is an adaptive benefit conferred by the proto-Kranz traits. Photosynthetic gas exchange responses demonstrate a subtle reduction of the CO<sub>2</sub> compensation point of photosynthesis ( $\Gamma$ ), which could provide slight yet biologically meaningful enhancements in carbon gain at low intercellular CO<sub>2</sub> levels. In *S. laxa*, the gas exchange benefits are a 5–7  $\mu\text{mol CO}_2 \text{ mol}^{-1}$  air reduction in  $\Gamma$  across a range of O<sub>2</sub> levels, and increased sensitivity of  $\Gamma$  to variation in light intensity (Morgan and Brown,

1980; Sage *et al.*, 2013). In *H. procumbens* and *H. karwinskyi*, the benefit may be a slight reduction in the slope of the  $\Gamma$  versus O<sub>2</sub> response (Vogan *et al.*, 2007). In *Flaveria pringlei* and *F. robusta*,  $\Gamma$  is also reduced by 5–10  $\mu\text{mol mol}^{-1}$  relative to the C<sub>3</sub> *F. cronquistii* and *Sartwellia flaveriae* (Sage *et al.*, 2013); however, no consistent gas exchange differences were observed in *Salsola montana* relative to its C<sub>3</sub> relatives (Voznesenskaya *et al.*, 2013). In *F. robusta*,  $\Gamma$  also exhibited greater light dependency than C<sub>3</sub> species (Sage *et al.*, 2013). Large reductions in  $\Gamma$  with an increase in light intensity indicate a C<sub>2</sub>-type of CCM may be active in higher plants (Sage *et al.*, 2013). The greater light dependency in *F. robusta* was associated with a shift to lower intercellular CO<sub>2</sub> values (C<sub>i</sub>) of the relationship between net CO<sub>2</sub> assimilation rate (*A*) and C<sub>i</sub>, which is not observed in the C<sub>3</sub> species, but is pronounced

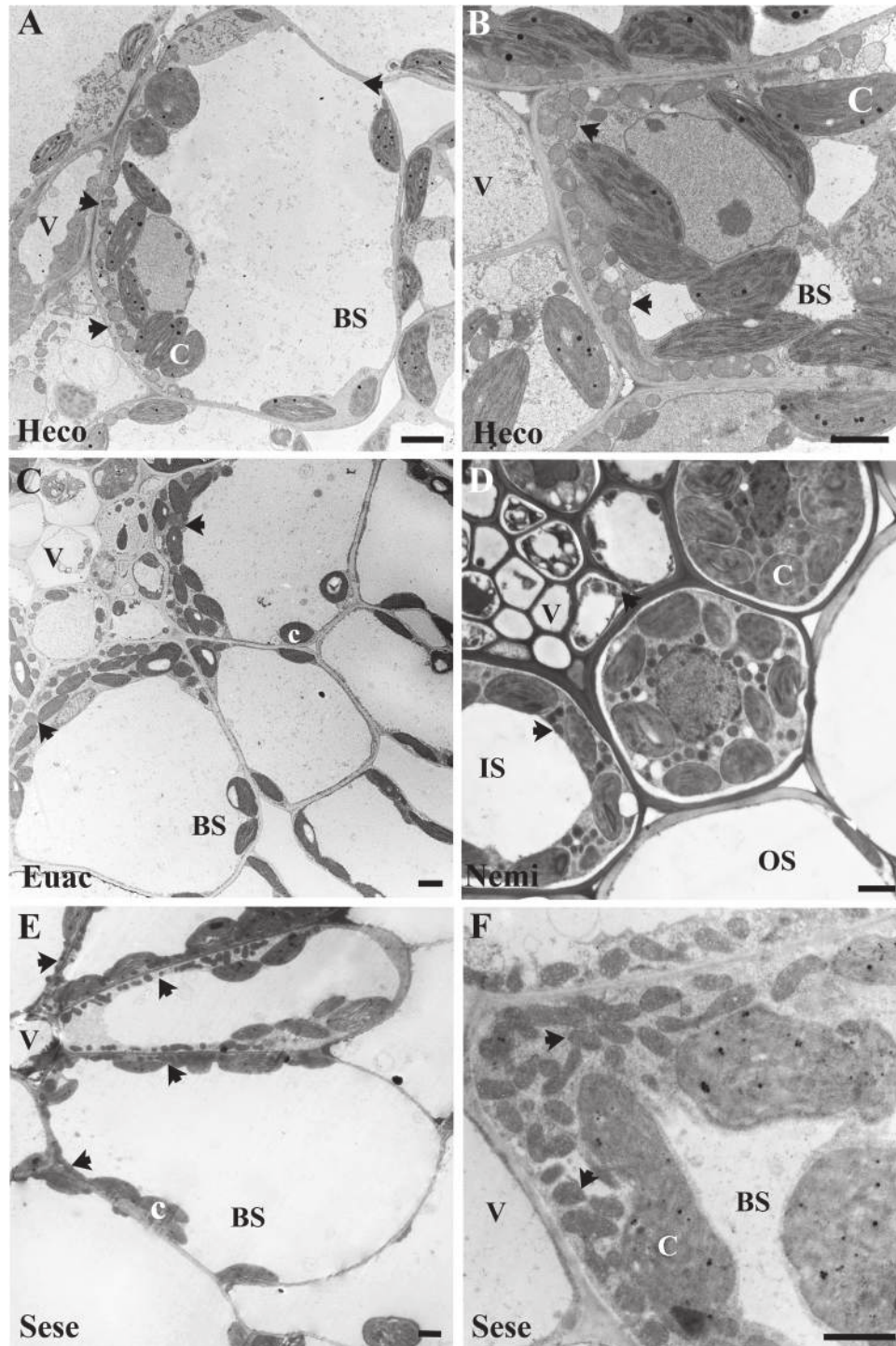


**Fig. 4.** The ultrastructure of bundle sheath cells in  $C_2$  species of *Heliotropium convolvulaceum* (Boraginaceae) at (A) low magnification and (B) high magnification; (C) *Euphorbia acuta* (Euphorbiaceae); (D) *Nuerachne minor* (Poaceae); and *Sedobassia sedoides* (Chenopodiaceae) at (E) low magnification and (F) high magnification. Bars=2  $\mu$ m.

in  $C_2$  species. This was interpreted by Sage et al., (2013) to indicate that *F. robusta* operates has a weak glycine shuttle which allows it to refix proportionally more photorespired  $CO_2$  than  $C_3$  species, although much less than in  $C_2$  species. This refixation mechanism may represent the adaptive benefit of the proto-Kranz suite of traits.

The refixation mechanism for photorespiratory  $CO_2$  in the proto-Kranz species may be nothing more than a single-cell

glycine shuttle within the BS that arises when mitochondria become localized to the inner BS wall (Fig. 2). Numerous chloroplasts remain against the outer perimeter of the cell facing the IAS, and thus are presumably assimilating  $CO_2$  and oxygenating RuBP. If the mitochondria have moved from a position near an outer chloroplast to the inner edge of the cell, any glycine formed during photorespiration would build up around the outer chloroplasts and diffuse to where GDC

is localized, which in the proto-Kranz species would be in the rank of mitochondria along the centripetal wall of the BS cells (Sage *et al.*, 2013). The diffusion barrier presented by the tonoplast and vacuole would then restrict the efflux of the photorespired CO<sub>2</sub>, causing it to accumulate and enhance photosynthesis within chloroplasts in the inner BS. It is also possible that the BS mitochondria receive glycine from the M tissue, which may happen in more than a trivial manner if photorespiration in the M cells exceeds the GDC capacity in the resident mitochondria. This could occur if the GDC capacity in M cells lags behind Rubisco oxygenase activity, which may happen in very hot climates during low CO<sub>2</sub> episodes, or if M GDC expression is reduced in proto-Kranz species. In either case, the increased number of BS mitochondria in proto-Kranz species indicates there is a rise in BS GDC capacity that might draw M glycine into the BS (Sage *et al.*, 2013). This would become an important source of CO<sub>2</sub> for the BS cells of the proto-Kranz species, and could establish conditions where additional reductions in M GDC allow for greater glycine flux to the BS, further enhancing carbon gain and thus facilitating positive selection for a stronger glycine shuttle (Sage *et al.*, 2012; Heckmann *et al.*, 2013).

The potential significance of the proto-Kranz traits is only recently recognized, and few species have been examined for this condition. It is possible that many species from hot climates have enlarged, activated bundle sheaths with a centripetal distribution of mitochondria. If this is the case, then there could be many possible candidates for evolving the two-tissue CCM of C<sub>2</sub> photosynthesis, and eventually, C<sub>4</sub> photosynthesis. Identification of additional proto-Kranz species will be essential for knowing whether the proto-Kranz condition is a common and perhaps essential early phase of C<sub>4</sub> evolution, and for studying the functional advantage of this trait.

## Kranz anatomy in C<sub>2</sub> plants

In contrast to the diversity observed in C<sub>4</sub> Kranz anatomy, Kranz-like anatomy in C<sub>2</sub> species is fairly homogeneous, in part because the known C<sub>2</sub> taxa are largely from clades with a similar leaf anatomy (Supplementary Fig. S2). For example, all but three of the identified C<sub>2</sub> species occur in eudicot clades where C<sub>4</sub> relatives express the Atriplicoid-type of Kranz anatomy, which is the most common type in C<sub>4</sub> dicots (Sage *et al.*, 2011a). Also, the physiological options for C<sub>2</sub> photosynthesis are fairly uniform compared with the possibilities for the C<sub>4</sub> pathway. In Type-I C<sub>2</sub> photosynthesis, Rubisco is both the primary carboxylase (in M cells) and secondary carboxylase (in BS cells), there is one decarboxylase (GDC), and the energetics of the M and BS chloroplasts are similar (von Caemmerer, 1989; Monson and Rawsthorne, 2000). Thus, certain factors that lead to biochemical and ultrastructural diversification between C<sub>4</sub> lineages do not seem to be major issues in C<sub>2</sub> evolution. The structural variation in C<sub>2</sub> anatomy that is most evident occurs in the Australian grass *Neurachne minor*, the only C<sub>2</sub> species in the *Neurachne* clade where C<sub>4</sub> evolution occurs twice, and in C<sub>2</sub> species in the Chenopodiaceae that are related to C<sub>4</sub> species with the Salsoloid-type of Kranz

anatomy (Hattersley *et al.*, 1986; Voznesenskaya *et al.*, 2001, 2013; Christin *et al.*, 2012). These variants are discussed below.

In most C<sub>2</sub> species, the distinguishing feature is a dense aggregation of chloroplasts and enlarged mitochondria along the inner periphery of the BS cells (Figs. 2, 4; Supplementary Fig. S2; Holaday *et al.*, 1984; Brown *et al.*, 1983; Moore *et al.*, 1987a; Hylton *et al.*, 1988; Brown and Hattersley, 1989; Monson and Rawsthorne, 2000; Christin *et al.*, 2011; Muhaidat *et al.*, 2011; Sage *et al.*, 2011b, 2012, 2013; Ueno *et al.* 2003; 2007; Voznesenskaya *et al.*, 2007, 2010, 2013). Glycine decarboxylase is abundant in these mitochondria, such that a dense band of immunolabel against GDC is observed along the inner BS of C<sub>2</sub> species in immunolocalization experiments (Fig. 3; Hylton *et al.*, 1988; Rawsthorne *et al.*, 1988; Ueno *et al.*, 2006; Voznesenskaya *et al.*, 2007; Muhaidat *et al.*, 2011; Sage *et al.*, 2011b, 2013). In the C<sub>2</sub> species with an inner rank of mitochondria, few if any mitochondria are present along the outer periphery of the cell (Muhaidat *et al.*, 2011; Sage *et al.*, 2011b, 2013; Voznesenskaya *et al.*, 2007, 2013). This polarity in mitochondrial placement is one of the distinguishing features in most of the C<sub>2</sub> species examined. The chloroplasts in the inner BS typically line up next to the rank of mitochondria (Figs 2, 4; Monson and Rawsthorne, 2000; Sage *et al.*, 2012; 2013). Rubisco and starch are abundant in these chloroplasts, and it is generally assumed they are photosynthetically engaged (Hylton *et al.*, 1988; Rawsthorne, 1992; Voznesenskaya *et al.*, 2001; Muhaidat *et al.*, 2011; Sage *et al.*, 2013). In many, but not all cases, the chloroplasts are abundant enough to form a near-continuous layer between the mitochondria and the vacuole (Holaday *et al.*, 1984; Brown and Hattersley, 1989; Muhaidat *et al.*, 2011; Sage *et al.*, 2013). This arrangement is particularly effective in enhancing the probability of photorespired CO<sub>2</sub> being captured and refixed by the inner chloroplasts before it can escape the cell (Rawsthorne, 1992). Many C<sub>2</sub> species also have chloroplasts along the outer BS periphery, but these are not associated with mitochondria as they are in C<sub>3</sub> species (Voznesenskaya *et al.*, 2007; 2010; 2013; Muhaidat *et al.*, 2011; Sage *et al.*, 2011b; Sage *et al.*, 2013). Hence, any photorespiratory metabolites produced by these chloroplasts will have to diffuse into the inner BS for metabolism.

Anatomically, the BS cells of C<sub>2</sub> species are generally more pronounced in leaf cross sections than they are in C<sub>3</sub> species, reflecting in most cases a larger BS cell size (Supplementary Fig. S2; McKown and Dengler 2007; Muhaidat *et al.*, 2011; Sage *et al.*, 2011b, 2013). With the pronounced clump of organelles lining the inner BS, the BS cells of C<sub>2</sub> species exhibit a modest wreath-like appearance that is apparent in cross sections and vein of leaf clearings, including leaves reconstituted from herbarium specimens (Supplementary Fig. S2; McKown and Dengler, 2007; Muhaidat *et al.*, 2011; Sage *et al.*, 2011b; Christin *et al.*, 2011; Khoshravesh *et al.*, 2012). This characteristic allows for relatively rapid screens for possible new C<sub>2</sub> species using herbarium material, which is important, as living C<sub>2</sub> plants are often unavailable. Carbon isotope screens do not generally identify C<sub>2</sub> species (Sage *et al.*, 2007). C<sub>2</sub> BS cells are rarely as distinctive as C<sub>4</sub> Kranz cells, which are more prominent owing to a larger and denser organelle mass (Figs 2, 4; supplementary Fig. S2).

In most C<sub>2</sub> species, the M tissue is reduced in prominence compared with C<sub>3</sub> relatives, as a result of larger BS cells and in many cases, greater vein density (Supplementary Fig. S2; Ueno *et al.* 2006; McKown and Dengler, 2007; Muhaidat *et al.*, 2011). However, unlike the case with C<sub>4</sub> Kranz, multiple layers of M cells remain around the BS cells and M:BS cell ratios rarely approach the low values observed in C<sub>4</sub> plants (McKown and Dengler, 2007, 2009; Voznesenskaya *et al.*, 2007, 2010, 2013). The ultrastructure of M cells of C<sub>2</sub> species changes little from their C<sub>3</sub> counterparts. C<sub>2</sub> and C<sub>3</sub> M cells of related plants have similar chloroplast numbers, distribution, and size (Stata *et al.*, 2014). GDC is often absent in the M cells, leading to the proposal that activation of the C<sub>2</sub> pathway follows a mutation that knocks out GDC expression in the M mitochondria (Monson and Rawsthorne 2000; Sage *et al.*, 2012). In *Cleome*, *Euphorbia*, *Heliotropium*, *Mollugo*, and *Portulaca*, there is no evidence for GDC expression in the M mitochondria of C<sub>2</sub> species (Marshall *et al.*, 2007; Muhaidat *et al.*, 2011; Sage *et al.*, 2011b; Voznesenskaya *et al.*, 2007, 2010). In *Flaveria*, however, the loss of GDC is gradual. C<sub>2</sub> *Flaveria* species branching lower in the phylogeny still express GDC protein and mRNA in the M mitochondria, whereas C<sub>2</sub> and C<sub>4</sub> *Flaveria* species branching in a more distal position have negligible GDC expression in M cells (Sage *et al.*, 2013; Schulze *et al.*, 2013).

The three exceptions to the typical C<sub>2</sub> Kranz anatomy described above are the grass *Neurachne minor*, two *Salsola* species of the Chenopodiaceae (*Sa. arbusculiformis* and *Sa. divaricata*) and the chenopod *Sedobassia sedoides*. In *N. minor*, the cells of an inner sheath that sit just inside a relatively empty outer sheath are co-opted to be the site of CO<sub>2</sub> concentration, and presumably, GDC localization (Fig. 4; Supplementary Fig. S2B; Hattersley *et al.*, 1986; Brown and Hattersley, 1989). In these cells, chloroplast and mitochondrial density are high, but there is no apparent pattern in their distribution (Fig. 4D). It is likely that the wall of the inner sheath, and the outer sheath layer of cells, provide a strong barrier to leakage of photorespired CO<sub>2</sub> such that the organelles need not be localized next to each other along the inner cell wall (Brown and Hattersley, 1989). In many succulent chenopods, the leaf anatomy is comprised of multiple layers of M cells around a central core of water storage cells (Voznesenskaya *et al.*, 2001, 2013). The inner M cell layer is co-opted as the site of CO<sub>2</sub> concentration in the C<sub>2</sub> chenopods and the C<sub>4</sub> species that have Salsaloid- and Kochioid-types of Kranz anatomy (Edwards and Voznesenskaya, 2011; Voznesenskaya *et al.*, 2001, 2013). In the C<sub>2</sub> species *Salsola arbusculiformis*, *Sa. divaricata*, and *Se. sedoides*, the inner Kranz-like layer where GDC is localized occurs adjacent to vascular cells along the periphery of the water storage cells, in what is interpreted to be an intermediate version of the Salsoloid Kranz anatomy (Voznesenskaya *et al.*, 2013; Freitag and Kadereit, 2013). In *Sa. arbusculiformis* and *Sa. divaricata*, the BS mitochondria and chloroplasts are very abundant, occupying over a third of the cell-volume (Voznesenskaya *et al.*, 2001, 2013). In *Se. sedoides*, many mitochondria line the BS walls adjacent to vascular tissue and other BS cells, but avoid the outer BS facing the intercellular air space (Fig. 4E, F).

The transition from proto-Kranz to C<sub>2</sub>-Kranz can be inferred in *Flaveria*, *Heliotropium* and *Steinchisma*, as indicated by the sister position of the proto-Kranz and C<sub>2</sub> species in their respective phylogenies. In *Salsola*, the proto-Kranz species *Sa. montana* is present on a close, yet separate branch of the phylogeny than the nearest known C<sub>2</sub> species (Voznesenskaya *et al.*, 2013). In *Flaveria* and *Heliotropium*, the changes are similar, being characterized by further enlargement of the BS tissue and increases in organelle size and number, resulting in more chloroplasts associating with the inner mitochondria (McKown and Dengler, 2007; Muhaidat *et al.*, 2011; Sage *et al.*, 2013). A reduction or loss of GDC expression is apparent in the M tissue, which when coupled with the larger and more numerous BS mitochondria, explains the reduction in the CO<sub>2</sub> compensation point to values that are half of the C<sub>3</sub> values (Muhaidat *et al.*, 2011; Sage *et al.*, 2013). In *Steinchisma*, the principal change between the proto-Kranz and C<sub>2</sub> species is an increase in chloroplast number and size in the inner BS region. Compared with the proto-Kranz *S. laxa*, the BS of the C<sub>2</sub> species *St. spathellosum* (formerly *Panicum schenckii*) has twice the number of mitochondria, 25% more chloroplasts, and three times as many peroxisomes; however, cell size does not differ (Brown *et al.*, 1983). In considering these examples, it is apparent that the formation of C<sub>2</sub> Kranz from the proto-Kranz condition requires multiple genetic changes and cannot be attributed to a single cause, such as GDC loss in the M tissue. GDC decline in M cells may be an important facilitator of the transition from proto-Kranz to C<sub>2</sub> Kranz, because it may establish a two-tissue glycine shuttle, with subsequent evolutionary selection creating the similar Kranz-like traits that occur repeatedly in the C<sub>2</sub> lineages (Sage *et al.*, 2012; Heckmann *et al.*, 2013; Schulze *et al.*, 2013). In any case, the multiple convergence on C<sub>2</sub> Kranz is strong evidence that this anatomy is specifically adapted for the C<sub>2</sub> pathway, in the same vein that C<sub>4</sub> Kranz is an adaptation for C<sub>4</sub> photosynthesis.

Within the C<sub>2</sub> condition, the major change is the shift from the Type I condition of C<sub>2</sub> photosynthesis only, to the Type II condition of C<sub>2</sub> photosynthesis and an accessory C<sub>4</sub> metabolic cycle (Edwards and Ku, 1987). In Type II species, the C<sub>4</sub> metabolic cycle can account for up to 50% percent of the initial carboxylation capacity, and reduce the CO<sub>2</sub> compensation point of photosynthesis to below 10 μmol mol<sup>-1</sup> (Moore *et al.*, 1987b; Monson *et al.*, 1988; Monson and Rawsthorne, 2000). However, there are no major structural changes associated with the transition from the Type I to Type II modes, and the C<sub>2</sub> Kranz type are similar in Type I and Type II forms, as indicated by studies with *Flaveria* and *Mollugo* (Kennedy *et al.*, 1980; Holaday *et al.*, 1984; Edwards and Ku, 1987; Monson and Rawsthorne, 2000).

## Kranz anatomy in C<sub>4</sub>-like plants

The C<sub>4</sub>-like condition is only confirmed in three species, all of which occur in *Flaveria* (*F. brownii*, *F. palmerii*, and *F. vaginata*; Monson *et al.*, 1987; Moore *et al.*, 1989; Ku *et al.* 1991); however, isotopic and anatomical evidence from herbarium specimens indicate additional C<sub>4</sub>-like species exist in *Blepharis*

(Acanthaceae; McDade, Sage, and Sage, unpublished) and *Anticharis* (Scrophulariaceae; Khoshnavesh *et al.*, 2012). Although the diversity of known C<sub>4</sub>-like species limits the ability to make broad inferences, the C<sub>4</sub>-like species of *Flaveria* are well studied and thus, for *Flaveria* at least, provide a detailed observation of the late stages of C<sub>4</sub> evolution. *Flaveria palmerii* and *F. vaginata* are in clade A where they are sister to the full C<sub>4</sub> species of *Flaveria*; *F. brownii* occurs on a distinct phylogenetic branch, termed clade B and lacks immediate C<sub>4</sub> relatives (McKown *et al.*, 2005). On both clades A and B, Type II C<sub>2</sub> species branch just below the C<sub>4</sub> like species, indicating the C<sub>4</sub>-like species arose from type II C<sub>2</sub> ancestors (McKown *et al.*, 2005).

The transition from Type II C<sub>2</sub> species to the C<sub>4</sub>-like condition is marked by a dramatic rise in the activity of the C<sub>4</sub> cycle enzymes, increased water- and Rubisco-use efficiency of photosynthesis, and a large reduction in Rubisco and C<sub>3</sub> cycle activity in the M cells (Fig. 2; Moore *et al.*, 1987b; Ku *et al.*, 1991; Dai *et al.*, 1996; Monson and Rawsthorne, 2000; Kocacinar *et al.*, 2008; Vogan and Sage, 2011). PEPC and NADP-ME activities, for example, are 5-fold higher in the C<sub>4</sub>-like species than the C<sub>2</sub> species and are similar to the C<sub>4</sub> values (Ku *et al.*, 1991). Also, in the C<sub>4</sub>-like species, the percentage of <sup>14</sup>C label present in aspartate and malate exceeds 67%, compared with 46% in the highest Type II C<sub>2</sub> species (Moore *et al.*, 1987b) and CO<sub>2</sub> compensation points drop to within a few μmol mol<sup>-1</sup> of C<sub>4</sub> values (Ku *et al.*, 1991; Dai *et al.*, 1996). These results demonstrate a strong enhancement of the C<sub>4</sub> metabolic cycle and corresponding reduction in the M C<sub>3</sub> cycle in what is considered to be the activation of the C<sub>4</sub> pathway (Sage *et al.*, 2012). C<sub>4</sub>-like plants are not considered to be fully developed C<sub>4</sub> species because the localization of Rubisco into the BS is incomplete, the oxygen inhibition of photosynthesis is halfway between C<sub>3</sub> and C<sub>4</sub> values, and the carbon isotope ratios are below the C<sub>4</sub> range, although they are higher than in most C<sub>3</sub> species (Monson *et al.*, 1988; Ku *et al.*, 1991; Monson and Rawsthorne, 2000). In addition, PEPC, Rubisco and carbonic anhydrase may not have fully evolved the kinetic and regulatory properties of the isoforms in their close C<sub>4</sub> relatives (Engelmann *et al.*, 2003; Ludwig, 2011; Ludwig, 2013). The acquisition of these final set of characteristics that distinguish an efficient, fully expressed C<sub>4</sub> pathway occur in a final phase of C<sub>4</sub> evolution termed the optimization phase (Sage *et al.*, 2012).

Structurally, the Kranz anatomy of the C<sub>4</sub>-like phase is best described in *F. brownii*. In *F. palmerii* and *F. vaginata*, the structural features are largely C<sub>4</sub> in nature and don't reveal much about the final phase before the acquisition of full C<sub>4</sub> Kranz anatomy (McKown and Dengler, 2007; Rahman, Sage, and Sage, unpublished). *Flaveria brownii* retains vestiges of the C<sub>2</sub> condition. The fraction of BS tissue in the leaf is also less in *F. brownii* than in C<sub>4</sub> leaves (Araus *et al.*, 1990). The bundle sheath ultrastructure of *F. brownii* is intermediate between Type II C<sub>2</sub> species and C<sub>4</sub> species: chloroplasts are larger and more numerous in *F. brownii* than in Type II species, but much shorter than in the C<sub>4</sub> *Flaveria* species such as *F. trinervia* (Fig. 2; Holaday *et al.*, 1984; Araus *et al.*, 1990). In *F. brownii*, many BS mitochondria occur along the interior of the centripetal wall of the BS cells, similar to the pattern

observed in C<sub>2</sub> species, but markedly different than in *F. trinervia*, where mitochondria do not form distinct ranks along the inner BS periphery (Fig. 2; Holaday *et al.*, 1984; Brown and Hattersley, 1989; Araus *et al.*, 1990). As with the biochemical and physiological responses, it is safe to conclude that the Kranz anatomy of *F. brownii* is intermediate between the C<sub>2</sub> and C<sub>4</sub> Kranz modes.

## Conclusion

Over the past 40 years, studies with species that exhibit intermediate traits support models that the evolution of C<sub>4</sub> photosynthesis is a staged affair, with the two-celled, photorespiratory glycine shuttle being a critical intermediate step. We propose here that there were four important events that facilitated the evolution of C<sub>4</sub> photosynthesis (Fig. 2). The first is the activation of the C<sub>3</sub> BS, such that in hot environments, high vein density and BS cells become photosynthetically engaged through greater exposure to intercellular air spaces and the acquisition of increased numbers of chloroplasts and mitochondria. These cells are completely C<sub>3</sub>, but their enhanced physiological activity enables the formation of weak mechanisms to scavenge photorespiratory CO<sub>2</sub> via the second key event, the migration of mitochondria to the centripetal region of the BS cells. With the reorientation of some chloroplasts to the inner wall to join the mitochondria the proto-Kranz condition arises, and with it, the potential to establish facilitation cascades where the M GDC is reduced while BS GDC and organelle numbers sequentially increase, activating the C<sub>2</sub> photorespiratory CCM. This reduction in M GDC represents the third major event in C<sub>4</sub> evolution. In time, key components of the C<sub>4</sub> metabolic cycle are up-regulated to complement C<sub>2</sub> photosynthesis, and this is proposed to facilitate the next major event, the activation of the full C<sub>4</sub> pathway with the coincident decline of the C<sub>3</sub> pathway in M tissues. Once the C<sub>4</sub>-like condition is achieved, evolutionary optimization adjusts many of the photosynthetic components to efficiently operate in the C<sub>4</sub> context, leading to fully developed C<sub>4</sub> photosynthesis. Many C<sub>3</sub>-C<sub>4</sub> species from 20 or so lineages support various aspects of this model, although our understanding of the initial and end phases are heavily dependent upon just a few species from a couple of lineages. These handful of species may skew our impression of early and late events, and thus it is important to use phylogenetic analyses to identify and collect addition proto-Kranz and C<sub>4</sub>-like species. By doing so, the amount of information available to parameterize models that can analyse and predict trajectories of C<sub>4</sub> evolution will substantially increase.

## Supplementary data

Supplementary data are available at *JXB* online

**Figure S1.** Transverse sections showing the leaf anatomy of three C<sub>4</sub> species and a C<sub>3</sub> species from the PACMAD clade of grasses, and C<sub>3</sub> and C<sub>4</sub> species from three C<sub>4</sub> lineages of the Chenopodiaceae.

**Figure S2.** Transverse sections illustrating leaf anatomy of closely related  $C_3$ ,  $C_2$ , and  $C_4$  species from six lineages of  $C_4$  photosynthesis, and a Canadian International Development Agency (CIDA) GCIAR-Canada linkage fund grant to TLS and RFS.

## Acknowledgements

The authors thank Kate Sault, Matt Stata, Stefanie Sultmanis, and Troy Rennie for technical assistance. This research was supported by grants from the Natural Science and Engineering Research Council of Canada (grant nos. 155258-2008 to TLS and 154273-2012 to RFS) and a Canadian International Development Agency (CIDA) GCIAR-Canada linkage fund grant to TLS and RFS.

## References

- Ackerly DD.** 1999. Comparative plant ecology and the role of phylogenetic information. In: Press MC, Scholes JD, Barker MG, eds. *Physiological plant ecology*. Oxford: Blackwell Science, 391–413.
- Aliscioni SS, Giussani LM, Zuloaga FO, Kellogg EA.** 2003. A molecular phylogeny of *Panicum* (Poaceae: Paniceae): tests of monophyly and phylogenetic placement within the Panicoideae. *American Journal of Botany* **90**, 796–821.
- Apel P, Horstmann C, Pfeffer M.** 1997. The *Moricandia* syndrome in species of the Brassicaceae - evolutionary aspects. *Photosynthetica* **33**, 205–215.
- Araus JL, Brown RH, Bouton J, Serret MD.** 1990. Inheritance of leaf anatomical characteristics in  $C_4$  *Flaveria* plants. *Photosynthesis Research* **26**, 49–57.
- Bauwe H.** 2011. Photorespiration: the bridge to  $C_4$  photosynthesis. In: Raghavendra AS, Sage RF, eds.  *$C_4$  photosynthesis and related  $CO_2$  concentrating mechanisms*, *Advances in Photosynthesis Vol. 32*. Heidelberg-Berlin: Springer Verlag, 81–108.
- Besnard G, Muasya AM, Russier F, Roalson EH, Salamin N, Christin P-A.** 2009. Phylogenomics of  $C_4$  photosynthesis in sedges (Cyperaceae): multiple appearances and genetic convergence. *Molecular Biology and Evolution* **26**, 1909–1919.
- Bissinger K, Khoshravesh R, Kotrade JP, Oakley J, Sage TL, Sage RF, Hartmann H, Kadereit G.** 2014. *Gisekia* (Gisekiaceae): phylogenetic relationships, biogeography, and ecophysiology of a poorly known  $C_4$  lineage in the Caryophyllales. *American Journal of Botany* **101**, 1–11.
- Botha CEJ.** 1992. Plasmodesmatal distribution, structure and frequency in relation to assimilation in  $C_3$  and  $C_4$  grasses in southern Africa. *Planta* **87**, 348–358.
- Bowes G.** 2011. Single-cell  $C_4$  photosynthesis in aquatic plants. In: Raghavendra AS, Sage RF, eds.  *$C_4$  photosynthesis and related  $CO_2$  concentrating mechanisms*, *Advances in Photosynthesis, Vol. 32*. Dordrecht: Springer, 63–80.
- Bräutigam A, Weber APM.** 2011. Transport processes: connecting the reactions of  $C_4$  photosynthesis. In: Raghavendra AS, Sage RF, eds.  *$C_4$  photosynthesis and related  $CO_2$  concentrating mechanisms*, *Advances in Photosynthesis, Vol. 32*. Dordrecht: Springer 199–219.
- Brown RH, Bouton JH, Rigsby L, Rigler M.** 1983. Photosynthesis of grass species differing in carbon-dioxide fixation pathways. VIII. Ultrastructural characteristics of *Panicum* species in the *laxa* group. *Plant Physiology* **71**, 425–431.
- Brown RH, Hattersley PW.** 1989. Leaf anatomy of  $C_3$ – $C_4$  species as related to evolution of  $C_4$  photosynthesis. *Plant Physiology* **91**, 1543–1550.
- Brown WV.** 1975. Variations in anatomy, associations, and origins of Kranz tissue. *American Journal of Botany* **62**, 395–402.
- Brown WV.** 1977. The Kranz syndrome and its subtypes in grass systematics. *Memoirs of the Torrey Botanical Club* **23**, 1–97.
- Busch FA, Sage TL, Cousins AB, Sage RF.** 2013.  $C_3$  plants enhance rates of photosynthesis by reassimilating photorespired and respired  $CO_2$ . *Plant, Cell and Environment* **36**, 200–212.
- Christin P-A, Osborne CP, Chatelet DS, Columbus JT, Besnard G, Hodkinson TR, Garrison LM, Vorontsova MS, Edwards EJ.** 2013. Anatomical enablers and the evolution of  $C_4$  photosynthesis. *Proceeding of the National Academy of Sciences, USA* **110**, 1381–1386.
- Christin P-A, Sage TL, Edwards EJ, Ogburn RM, Khoshravesh R, Sage RF.** 2011. Complex evolutionary transitions and the significance of  $C_3$ – $C_4$  intermediate forms of photosynthesis in Molluginaceae. *Evolution* **65**, 643–660.
- Christin P-A, Wallace MJ, Clayton H, Edwards EJ, Furbank, Hattersley PW, Sage RF, MacFarlane TD, Ludwig M.** 2012. Multiple photosynthetic transitions, polyploidy and lateral gene transfer in the grass subtribe Neurachninae. *Journal of Experimental Botany* **63**, 6297–6308.
- Covshoff S, Burgess SJ, Kneřová J, and Kümpers BM.** 2014. Getting the most out of natural variation in  $C_4$  photosynthesis. *Photosynthesis Research* **119**, 157–167.
- Covshoff S, Furbank RT, Leegood RC, Hibberd JM.** 2012. Leaf rolling allows quantification of mRNA abundance in mesophyll cells of sorghum. *Journal of Experimental Botany* **64**, 807–813.
- Covshoff S, Hibberd JM.** 2012. Integrating  $C_4$  photosynthesis into  $C_3$  crops to increase yield potential. *Current Opinion in Biotechnology* **23**, 209–214.
- Dai ZY, Ku MSB, Edwards GE.** 1996. Oxygen sensitivity of photosynthesis and photorespiration in different photosynthetic types in the genus *Flaveria*. *Planta* **198**, 563–571.
- Dengler NG, Nelson T.** 1999. Leaf structure and development in  $C_4$  plants. In: Sage R, Monson R, eds.  *$C_4$  plant biology*. San Diego: Academic Press, 133–172.
- Djamali M, Brewer S, Breckle S, Jackson ST.** 2012. Climatic determinism in phytogeographic regionalization: A test from the Irano-Turanian region, SW and Central Asia. *Flora* **207**, 237–249.
- Edwards EJ, Osborne CP, Stromberg CAE, Smith SA, Consortium CG.** 2010. The origins of  $C_4$  grasslands: integrating evolutionary and ecosystem science. *Science* **328**, 587–91.
- Edwards GE, Ku MSB.** 1987. Biochemistry of  $C_3$ – $C_4$  intermediates. In: MD Hatch, NK Boardman, eds. *Biochemistry of Plants: Photosynthesis, Vol. 14*. San Diego: Academic Press 275–325.
- Edwards GE, Voznesenskaya EV.** 2011. Kranz forms and single cell  $C_4$  in terrestrial plants. In: Raghavendra AS, Sage RF, eds.  *$C_4$  photosynthesis and related  $CO_2$  concentrating mechanisms*, *Advances in Photosynthesis Vol. 32*. Heidelberg-Berlin: Springer Verlag, 29–61.
- Engelmann S, Bläsing OE, Gowik U, Svensson P, Westhoff P.** 2003. Molecular evolution of  $C_4$  phosphoenolpyruvate carboxylase in the genus *Flaveria* - a gradual increase from  $C_3$  to  $C_4$  characteristics. *Planta* **217**, 717–725.
- Evert RF, Eschrich W, Heyser W.** 1977. Distribution and structure of the plasmodesmata in mesophyll and bundle-sheath cells of *Zea mays* L. *Planta* **136**, 77–89.
- Feodorova TA, Voznesenskaya EV, Edwards GE, Roalson EH.** 2010. Biogeographic patterns of diversification and the origins of  $C_4$  in *Cleome* (Cleomaceae). *Systematic Botany* **35**, 811–826.
- Fouracre JP, Ando S, Langdale JA.** 2014. Cracking the Kranz enigma with systems biology. *Journal of Experimental Botany* **65**, 3327–3339.
- Freitag H, Kadereit G.** 2013.  $C_3$  and  $C_4$  leaf anatomy types in Camphorosmeae (Camphorosmoideae, Chenopodiaceae). *Plant Systematics and Evolution* doi 10.1007/s00606-013-0912-9.
- Frohlich MW.** 1978. *Systematics of Heliotropium section Orthostachys in Mexico*. PhD thesis, Cambridge, Massachusetts: Harvard University.
- Furbank RT.** 2011. Evolution of  $C_4$  photosynthetic mechanism: are there really three  $C_4$  acid decarboxylation types? *Journal of Experimental Botany* **62**, 3103–3108.
- Gowik U, Westhoff P.** 2011.  $C_4$ -phosphoenolpyruvate carboxylase. In: Raghavendra AS, Sage RF, eds.  *$C_4$  photosynthesis and related  $CO_2$  concentrating mechanisms*, *Advances in Photosynthesis, Vol. 32*. Dordrecht, The Netherlands: Springer, 257–275.
- Grass Phylogeny Working Group II.** 2012. New grass phylogeny resolves deep evolutionary relationships and discovers  $C_4$  origins. *New Phytologist* **193**, 304–312.
- Griffiths H, Weller G, Toy LF, Dennis RJ.** 2013. You're so vein: bundle sheath physiology, phylogeny and evolution in  $C_3$  and  $C_4$  plants. *Plant, Cell and Environment* **36**, 249–261.
- Haberlandt G.** 1914. *Physiological Plant Anatomy*. Macmillan, London.

- Hatch MD.** 1987. C<sub>4</sub> photosynthesis: a unique blend of modified biochemistry, anatomy and ultrastructure. *Biochimica et Biophysica Acta* **895**, 81–106.
- Hattersley PW.** 1984. Characterization of C<sub>4</sub> type leaf anatomy in grasses (Poaceae). Mesophyll:bundle sheath area ratios. *Annals of Botany* **53**, 163–179.
- Hattersley PW, Browning AJ.** 1981. Occurrence of the suberized lamella in leaves of grasses of different photosynthetic types. I. In parenchymatous bundle sheaths and PCR (“Kranz”) sheaths. *Protoplasma* **109**, 371–401.
- Hattersley PW, Watson L.** 1992. Diversification of photosynthesis. In: Chapman GP, ed. *Grass evolution and domestication*. London: Academic Press, 38–116.
- Hattersley PW, Watson L, Johnston CR.** 1982. Remarkable leaf anatomical variations in *Neurachne* and its allies (Poaceae) in relation to C<sub>3</sub> and C<sub>4</sub> photosynthesis. *Botanical Journal of the Linnean Society* **84**, 265–272.
- Hattersley PW, Wong SC, Perry S, Roksandic Z.** 1986. Comparative ultrastructure and gas-exchange characteristics of the C<sub>3</sub>–C<sub>4</sub> intermediate *Neurachne minor* S. T. Blake (Poaceae). *Plant, Cell and Environment* **9**, 217–233.
- Heckmann D, Schulze S, Denton A, Gowik U, Westhoff P, Andreas PM, Lercher MJ.** 2013. Predicting C<sub>4</sub> photosynthesis evolution: modular, individually adaptive steps on a Mount Fuji fitness landscape. *Cell* **153**, 1579–1588.
- Holaday AS, Black CC.** 1981. Comparative characterization of phosphoenolpyruvate carboxylase in C<sub>3</sub>, C<sub>4</sub> and C<sub>3</sub>–C<sub>4</sub> intermediate *Panicum* species. *Plant Physiology* **67**, 330–334.
- Holaday AS, Chollet R.** 1984. Photosynthetic/photorespiratory characteristics of C<sub>3</sub>–C<sub>4</sub> intermediate species. *Photosynthesis Research* **5**, 307–323.exas
- Holaday AS, Lee KW, Chollet R.** 1984. C<sub>3</sub>–C<sub>4</sub> intermediate species in the genus *Flaveria*: leaf anatomy, ultrastructure, and the effect of O<sub>2</sub> on the CO<sub>2</sub> compensation concentration. *Planta* **160**, 25–32.
- Hylton CM, Rawsthorne S, Smith AM, Jones DA, Woolhouse HW.** 1988. Glycine decarboxylase is confined to the bundle sheath cells of leaves of C<sub>3</sub>–C<sub>4</sub> intermediate species. *Planta* **175**, 452–459.
- Kadereit G, Ackerly D, Pirie MD.** 2012. A broader model for C<sub>4</sub> photosynthesis evolution in plants inferred from the goosefoot family (Chenopodiaceae s.s.). *Proceeding of the Royal Society, Biological Science* **279**, 3304–3311.
- Kadereit G, Freitag H.** 2011. Molecular phylogeny of Camphorosmeae (Camphorosmoideae, Chenopodiaceae): Implications for biogeography, evolution of C<sub>4</sub> photosynthesis and taxonomy. *Taxon* **60**, 51–78.
- Keeley JE.** 1990. Photosynthetic pathways in freshwater aquatic plants. *Trends in Ecology and Evolution* **5**, 330–333.
- Kennedy RA, Eastburn KL, Jensen KG.** 1980. C<sub>3</sub>–C<sub>4</sub> photosynthesis in the genus *Mollugo*: structure, physiology and evolution of intermediate characteristics. *American Journal of Botany* **67**, 1207–1217.
- Khoshravesh R, Akhani H, Sage TL, Nordenstam B, Sage RF.** 2012. Phylogeny and photosynthetic pathway distribution in *Anticharis* Endl. (Scrophulariaceae). *Journal of Experimental Botany* **63**, 5645–5658.
- Kocacinar F, McKown AD, Sage TL, Sage RF.** 2008. Photosynthetic pathway influences xylem structure and function in *Flaveria* (Asteraceae). *Plant, Cell and Environment* **31**, 1363–1376.
- Koteyeva NK, Voznesenskaya EV, Roalson EH, Edwards GE.** 2011. Diversity in forms of C<sub>4</sub> in the genus *Cleome* (Cleomaceae). *Annals of Botany* **107**, 269–283.
- Ku MSB, Wu J, Dai Z, Scott RA, Chu C, Edwards GE.** 1991. Photosynthetic and photorespiratory characteristics of *Flaveria* species. *Plant Physiology* **96**, 518–528.
- Laetsch WM.** 1974. The C<sub>4</sub> syndrome: a structural analysis. *Annual Review Plant Physiology* **25**, 27–52.
- Ludwig M.** 2011. The molecular evolution of β-carbonic anhydrase in *Flaveria*. *Journal of Experimental Botany* **62**, 3071–3081.
- Ludwig M.** 2013. Evolution of the C<sub>4</sub> photosynthetic pathway: events at the cellular and molecular levels. *Photosynthesis Research* **117**, 147–161.
- Marshall DM, Muhaidat R, Brown NJ, Liu Z, Griffiths H, Sage RF, Hibberd JM.** 2007. *Cleome*, a genus closely related to *Arabidopsis*, contains species spanning a developmental progression from C<sub>3</sub> to C<sub>4</sub> photosynthesis. *Plant Journal* **51**, 886–896.
- McKown AD, Dengler NG.** 2007. Key innovations in the evolution of Kranz anatomy and C<sub>4</sub> vein pattern in *Flaveria* (Asteraceae). *American Journal of Botany* **94**, 382–399.
- McKown AD, Dengler NG.** 2009. Shifts in leaf vein density through accelerated vein formation in C<sub>4</sub> *Flaveria* (Asteraceae). *Annals of Botany* **104**, 1085–1098.
- McKown AD, Moncalvo JM, Dengler NG.** 2005. Phylogeny of *Flaveria* (Asteraceae) and inference of C<sub>4</sub> photosynthesis evolution. *American Journal of Botany* **92**, 1911–1928.
- Mertz RA, Brutnell TP.** 2014. Bundle sheath suberization in grass leaves: multiple barriers to characterization. *Journal of Experimental Botany* **65**, 3371–3380.
- Metcalfe CR, Chalk L.** 1979. *Anatomy of the Dicotyledons, Second Edition, Volume 1: Systematic Anatomy of the Leaf and Stem*. Oxford: Oxford University Press.
- Monson RK.** 1989. On the evolutionary pathways resulting in C<sub>4</sub> photosynthesis and Crassulacean acid metabolism. *Advances in Ecological Research* **19**, 57–110.
- Monson RK.** 1999. The origins of C<sub>4</sub> genes and evolutionary pattern in the C<sub>4</sub> metabolic phenotype. In: Sage R, Monson R, eds. *C4 Plant Biology*. San Diego: Academic Press, 337–410.
- Monson RK, Edwards GE, Ku MSB.** 1984. C<sub>3</sub>–C<sub>4</sub> intermediate photosynthesis in plants. *Bioscience* **34**, 563–571.
- Monson RK, Moore BD.** 1989. On the significance of C<sub>3</sub>–C<sub>4</sub> intermediate photosynthesis to the evolution of C<sub>4</sub> photosynthesis. *Plant, Cell and Environment* **12**, 689–699.
- Monson RK, Rawsthorne S.** 2000. Carbon dioxide assimilation in C<sub>3</sub>–C<sub>4</sub> intermediate plants. In: Leegood R, Sharkey T, Von Caemmerer S, eds. *Photosynthesis: physiology and metabolism*. *Advances in Photosynthesis*, Vol. **9**. Dordrecht: Kluwer Academic Press, 533–550.
- Monson RK, Schuster WS, Ku MSB.** 1987. Photosynthesis in *Flaveria brownii* A.M. Powell, a C<sub>4</sub>-like C<sub>3</sub>–C<sub>4</sub> intermediate. *Plant Physiology* **85**, 1063–1067.
- Monson RK, Teeri JA, Ku MSB, Gurevitch J, Mets LJ, Dudley S.** 1988. Carbon-isotope discrimination by leaves of *Flaveria* species exhibiting different amounts of C<sub>3</sub>- and C<sub>4</sub>-cycle cofunction. *Planta* **174**, 145–151.
- Moore BD, Franceschi VR, Cheng SH, Wu JR, Ku MSB.** 1987a. Photosynthetic characteristics of the C<sub>3</sub>–C<sub>4</sub> intermediate *Parthenium hysterophorus*. *Plant Physiology* **85**, 978–983.
- Moore BD, Ku MSB, Edwards GE.** 1987b. C<sub>4</sub> photosynthesis and light-dependent accumulation of inorganic carbon in leaves of C<sub>3</sub>–C<sub>4</sub> and C<sub>4</sub> *Flaveria* species. *Australian Journal of Plant Physiology* **14**, 657–668.
- Moore BD, Ku MSB, Edwards GE.** 1989. Expression of C<sub>4</sub>-like photosynthesis in several species of *Flaveria*. *Plant, Cell and Environment* **12**, 541–549.
- Morgan JA, Brown RH.** 1980. Photosynthesis in grass species differing in carbon dioxide fixation pathways. III. Oxygen response and enzyme activities of the *Laxa* groups of *Panicum*. *Plant Physiology* **65**, 156–159.
- Muhaidat R, Sage RF, Dengler NG.** 2007. Diversity of Kranz anatomy and biochemistry in C<sub>4</sub> eudicots. *American Journal of Botany* **94**, 362–381.
- Muhaidat R, Sage TL, Frohlich MW, Dengler NG, Sage RF.** 2011. Characterization of C<sub>3</sub>–C<sub>4</sub> intermediate species in the genus *Heliotropium* L. (Boraginaceae): anatomy, ultrastructure and enzyme activity. *Plant, Cell and Environment* **34**, 1723–1736.
- Oakley JC, Sultman S, Stinson CR, Sage TL, Sage RF.** 2014. Comparative studies of C<sub>3</sub> and C<sub>4</sub> *Atriplex* hybrids in the genomics era: physiological assessments. *Journal of Experimental Botany* **65**, 3637–3647.
- Ocampo G, Koteyeva NK, Voznesenskaya EV, Edwards GE, Sage TL, Sage RF, Columbus JT.** 2013. Evolution of leaf anatomy and photosynthetic pathways in Portulacaceae. *American Journal of Botany* **100**, 2388–2402.
- Osborne CP, Sack L.** 2012. Evolution of C<sub>4</sub> plants: a new hypothesis for an interaction of CO<sub>2</sub> and water relations mediated by plant hydraulics. *Philosophical Transactions of the Royal Society, Biological Science* **367**, 583–600.

- Pyankov VI, Voznesenskaya EV, Kuzmin AN, Ku MSB, Ganko E, Franceschi VR, Black CC, Edwards GE.** 2000. Occurrence of  $C_3$  and  $C_4$  photosynthesis in cotyledons and leaves of *Salsola* species (Chenopodiaceae). *Photosynthesis Research* **63**, 69–84.
- Rajendrudu G, Prasad JSR, Das VSR.** 1986.  $C_3$ – $C_4$  intermediate species in *Alternanthera* (Amaranthaceae) - leaf anatomy,  $CO_2$  compensation point, net  $CO_2$  exchange and activities of photosynthetic enzymes. *Plant Physiology* **80**, 409–414.
- Rawsthorne S.** 1992.  $C_3$ – $C_4$  intermediate photosynthesis: linking physiology to gene expression. *Plant Journal* **2**, 267–274.
- Rawsthorne S, Bauwe H.** 1998.  $C_3$ – $C_4$  intermediate photosynthesis. In: Raghavendra AS, eds. *Photosynthesis. A comprehensive treatise*. Cambridge: Cambridge University Press, 150–162.
- Rawsthorne S, Hylton CM, Smith AM, Woolhouse HW.** 1988. Photorespiratory metabolism and immunogold localization of photorespiratory enzymes in leaves of  $C_3$  and  $C_3$ – $C_4$  intermediate species of *Moricandia*. *Planta* **173**, 298–308.
- Roalson EH.** 2011.  $C_4$  photosynthesis origins in the monocots: a review and reanalysis. In: Raghavendra AS, Sage RF, eds.  *$C_4$  photosynthesis and related  $CO_2$  concentrating mechanisms*, *Advances in Photosynthesis Vol. 32*. Dordrecht: Springer, 319–338.
- Roalson EH, Hinchliff CE, Trevisan R, da Silva CRM.** 2010. Phylogenetic relationships in *Eleocharis* (Cyperaceae):  $C_4$  photosynthesis origins and patterns of diversification in the spikerushes. *Systematic Botany* **35**, 257–271.
- Roth-Nebelsick A, Uhl D, Mosbrugger V, Kerp H.** 2001. Evolution and function of leaf venation architecture: a review. *Annals of Botany* **87**, 553–566.
- Sabale AB, Bhosale LJ.** 1984.  $C_3$ – $C_4$  photosynthesis in *Bougainvillea* cv. Palmer, Mary. *Photosynthetica* **18**, 84–89.
- Sage RF.** 2001. Environmental and evolutionary preconditions for the origin and diversification of the  $C_4$  photosynthesis syndrome. *Plant Biology* **3**, 202–213.
- Sage RF.** 2002. Are CAM and  $C_4$  photosynthesis incompatible? *Australian Journal of Plant Physiology* **29**, 775–785.
- Sage RF.** 2004. The evolution of  $C_4$  photosynthesis. *New Phytologist* **161**, 341–370.
- Sage RF.** 2013. Photorespiratory compensation: a driver for biological diversity. *Plant Biology* **15**, 624–638.
- Sage TL, Busch FA, Johnson DC, Friesen PC, Stinson CR, Stata M, Sultmanis S, Rahman BA, Rawsthorne S, Sage RF.** 2013. Initial events during the evolution of  $C_4$  photosynthesis in  $C_3$  species of *Flaveria*. *Plant Physiology* **163**, 1266–1276.
- Sage RF, Christin P A, Edwards E J.** 2011a. The  $C_4$  plant lineages of planet Earth. *Journal of Experimental Botany* **62**, 3155–3169.
- Sage RF, Li MR, Monson RK.** 1999. The taxonomic distribution of  $C_4$  photosynthesis. In: Sage R, Monson RK, eds.  *$C_4$  plant Biology*. San Diego: Academic Press, 551–584.
- Sage RF, Sage TL, Kocacinar F.** 2012. Photorespiration and the evolution of  $C_4$  photosynthesis. *Annual Review of Plant Biology* **63**, 19–47.
- Sage RF, Sage TL, Pearcy RW, Borsch T.** 2007. The taxonomic distribution of  $C_4$  photosynthesis in Amaranthaceae *sensu stricto*. *American Journal of Botany* **94**, 1992–2003.
- Sage TL, Sage RF, Vogan PJ, Rahman B, Johnson DC, Oakley JC, Heckel MA.** 2011b. The occurrence of  $C_2$  photosynthesis in *Euphorbia* subgenus *Chamaesyce* (Euphorbiaceae). *Journal of Experimental Botany* **62**, 3183–3195.
- Schulze S, Mallmann J, Burscheidt J, Koczor M, Streubel M, Bauwe H, Gowik U, Westhoff P.** 2013. Evolution of  $C_4$  photosynthesis in the genus *Flaveria*: Establishment of a photorespiratory  $CO_2$  pump. *The Plant Cell* **25**, 2522–2535.
- Slewinski TL.** 2013. Using evolution as a guide to engineer Kranz-type  $C_4$  photosynthesis. *Frontiers in Plant Science* **4**, 1–13.
- Smith JAC, Winter K.** 1996. Taxonomic distribution of crassulacean acid metabolism. In: Winter K, Smith JAC, eds. *Crassulacean acid metabolism: biochemistry, ecophysiology and evolution*. Berlin: Springer-Verlag, 427–436.
- Soros CL, Dengler NG.** 2001. Ontogenetic derivation and cell differentiation in photosynthetic tissues of  $C_3$  and  $C_4$  species of the Cyperaceae. *American Journal of Botany* **88**, 992–1005.
- Stata M, Sage TL, Rennie TD, Khoshravesh R, Sultmanis S, Khaikin Y, Ludwig M, Sage RF.** 2014. Mesophyll cells of  $C_4$  plants have fewer chloroplasts than those of closely related  $C_3$  plants. *Plant Cell and Environment*. doi: 10.1111/pce.12331.
- Ueno O, Bang SW, Wada Y, Kobayashi N, Kaneko R, Kaneko Y, Matsuzawa Y.** 2007. Inheritance of  $C_3$ – $C_4$  intermediate photosynthesis in reciprocal hybrids between *Moricandia arvensis* ( $C_3$ – $C_4$ ) and *Brassica oleracea* ( $C_3$ ) that differ in genome constitution. *Plant Production Science* **10**, 68–79.
- Ueno O, Bang SW, Wada Y, Kondo A, Ishihara K, Kaneko Y, Matsuzawa Y.** 2003. Structural and biochemical dissection of photorespiration in hybrids differing in genome constitution between *Diplotaxis tenuifolia* ( $C_3$ – $C_4$ ) and Radish ( $C_3$ ). *Plant Physiology* **132**, 1550–1559.
- Ueno O, Wada Y, Wakai M, Bang SW.** 2006. Evidence from photosynthetic characteristics for the hybrid origin of *Diplotaxis muralis* from a  $C_3$ – $C_4$  intermediate and a  $C_3$  species. *Plant Biology* **8**, 253–259.
- Vogan PJ, Frohlich MW, Sage RF.** 2007. The functional significance of  $C_3$ – $C_4$  intermediate traits in *Heliotropium* L. (Boraginaceae): gas exchange perspective. *Plant, Cell and Environment* **30**, 1337–1345.
- Vogan PJ, Sage RF.** 2011. Water-use efficiency and nitrogen-use efficiency of  $C_3$ – $C_4$  intermediate species of *Flaveria* Juss. (Asteraceae). *Plant, Cell and Environment* **34**, 1415–1430.
- von Caemmerer S.** 1989. A model of photosynthetic  $CO_2$  assimilation and carbon-isotope discrimination in leaves of certain  $C_3$ – $C_4$  intermediates. *Planta* **178**, 463–474.
- von Caemmerer SV.** 2000. *Biochemical models of leaf photosynthesis*. CSIRO Publishing, Australia.
- von Caemmerer C, Furbank R.** 2003. The  $C_4$  pathway: an efficient  $CO_2$  pump. *Photosynthesis Research* **77**, 191–207.
- Voznesenskaya EV, Artyusheva EG, Franceschi VR, Pyankov VI, Kiirats O, Ku MSB, Edwards GE.** 2001. *Salsola arbusculiformis*, a  $C_3$ – $C_4$  Intermediate in Salsoleae (Chenopodiaceae). *Annals of Botany* **88**, 337–348.
- Voznesenskaya EV, Franceschi VR, Pyankov VI, Edwards GE.** 1999. Anatomy, chloroplast structure and compartmentation of enzymes relative to photosynthetic mechanisms in leaves and cotyledons of species in the tribe Salsoleae (Chenopodiaceae). *Journal of Experimental Botany* **50**, 1779–1795.
- Voznesenskaya EV, Gamaley YV.** 1986. The ultrastructural characteristics of leaf types with Kranz-anatomy. *Botanicheskii Zhurnal* **71**, 1291–1307. (In Russian).
- Voznesenskaya EV, Koteyeva NK, Akhiani H, Roalson EH, Edwards GE.** 2013. Structural and physiological analyses in Salsoleae (Chenopodiaceae) indicate multiple transitions among  $C_3$ , intermediate and  $C_4$  photosynthesis. *Journal of Experimental Botany* **64**, 3583–3604.
- Voznesenskaya EV, Koteyeva NK, Chuong SDX, Ivanova AN, Barroca J, Craven LA, Edwards GE.** 2007. Physiological, anatomical and biochemical characterisation of photosynthetic types in genus *Cleome* (Cleomaceae). *Functional Plant Biology* **34**, 247–267.
- Voznesenskaya EV, Koteyeva NK, Edwards GE, Ocampo G.** 2010. Revealing diversity in structural and biochemical forms of  $C_4$  photosynthesis and a  $C_3$ – $C_4$  intermediate in genus *Portulaca* L. (Portulacaceae). *Journal of Experimental Botany* **61**, 3647–3662.
- Williams BP, Johnston IG, Covshoff S, Hibberd JM.** 2013. Phenotypic landscape inference reveals multiple evolutionary paths to  $C_4$  photosynthesis. *eLife* **2**, e00961.
- Yang Y, Berry PE.** 2011. Phylogenetics of the Chamaesyce clade (*Euphorbia*, Euphorbiaceae): reticulate evolution and long-distance dispersal in a prominent  $C_4$  lineage. *American Journal of Botany* **98**, 1486–1503.